Elsevier Editorial System(tm) for Earth and Planetary Science Letters

Manuscript Draft

Manuscript Number: EPSL-D-18-00508R1

Title: Electrolytic Fluid Speciation by Gibbs Energy Minimization and Implications for Subduction Zone Mass Transfer

Article Type: Letters

Keywords: Electrolytic fluid speciation; Gibbs energy minimization; subduction; devolatilization; mass transfer; decarbonation

Corresponding Author: Dr. James A.D. Connolly,

Corresponding Author's Institution:

First Author: James A.D. Connolly

Order of Authors: James A.D. Connolly; Matthieu E Galvez

Abstract: The number of solute species required to describe the thermodynamic behavior of electrolytic fluids is a hindrance to the incorporation of aqueous geochemistry in petrological Gibbs energy minimization procedures. An algorithm is developed to overcome this problem. Beginning from the solute-free limit, chemical potentials, and phase stability are determined by minimization, the solute speciation and bulk fluid properties consistent with these chemical potentials are then computed and the procedure repeated until the chemical potentials converge. Application of the algorithm to a model for metamorphism of subducted sediment shows that accounting for solute chemistry does not change the conclusion based on molecular fluid models that a pervasive water flux from the subjacent mantle is required to explain island-arc carbon emissions by fluid-mediated slab decarbonation. This putative flux would deplete the sediment in potassium, limiting the capacity of the slab to transport water to greater depth and rendering it refractory to melting.

ETH
Eidgenössische Technische Hochschule Zürich
Swiss Federal Institute of Technology Zurich

Institut für Geochemie und Petrologie

ETH Zentrum
CH-8092 Zürich

Tel. +41-44-632 78 04
Fax +41-44-632 16 36
james.connolly@erdw.ethz.ch

July 20, 2018

Dear Mike:

Thank you for your care of my manuscript. If my revisions are otherwise acceptable, then I would like to add Matthieu Galvez as a coauthor. There are many reasons I believe the addition is justified, chief among them is that I cannot adequately acknowledge the importance of his motivational role with a simple statement in the acknowledgements. Matthieu has read the manuscript and agreed to be a coauthor. I apologize for any increase editorial overhead.

My revisions account for most of the comments made by you and Craig. The exception is that I have not included benchmark calculations, which are also suggested by the anonymous reviewer. Aside from my reluctance to spend time learning how to use other codes, the reason for my stubbornness is that, given the demonstrably limited capabilities of other codes, comparisons would need to be done on simplified systems. I prefer to highlight the practical capabilities of my own code, which, I am reasonably confident, are currently unequalled. The anonymous reviewer also requests more discussion of algorithms. I did not accede to this request because, as I mentioned in my original cover letter, for the majority of the EPSL readership algorithmic and practical capabilities bear no relationship to each other and it is the latter that are of interest.

Neither Craig nor the anonymous reviewer was particularly interested in criticizing my “application of scientific interest” and they both observe, and I concede, that the connection is rough. Despite this roughness, my opinion is that without an application the paper would be unsuitable for EPSL and that, without the algorithm, the scientific application could only be published with needless padding. Re the application, two readers of the manuscript, Galvez and Plank, came to perfectly opposed conclusions about whether my intention was to advocate or deny slab-melting when in fact it was neither. In an effort to avoid such confusion, I have moved the final two paragraphs of the original discussion into a “Conclusion” and added an intermediate paragraph to clarify my reasoning.

As things stand, I am fairly certain you were the only reader to have weighed both halves of the paper. Therefore, while I do not hope for a negative opinion, I would value it.

Best regards, Jamie.

Revision Notes

Ms. Ref. No.: EPSL-D-18-00508
Title: Electrolytic Fluid Speciation by Gibbs Energy Minimization and Implications for Subduction Zone Mass Transfer
Earth and Planetary Science Letters

Dear Jamie,

Obviously we will publish this paper but the key questions are how you make it suitably accessible to the readers. I enjoyed tha aplication to subduction zones and the review of C release. My feeling is that you could expand the discussion of the lagged speciation algorithm to make it more accessible. I got lost between equations 2 & 3 - I must be misunderstanding something simple here!

The step between eqs 2 & 3 is clarified by an intermediate equation.

Likewise line 112 'Regardless of those details, the flaw in this method is that if the solvent composition is consistent with the specified chemical potentials, as is the case when the chemical potentials and solvent composition are obtained by Gibbs energy inimization, then finite solute concentrations violate this consistency.' is obviously critical - I think I understand what you are saying but a more explicit explanation would be good.

The implication of the flaw, that there is no consistent relationship between the computed fluid speciation and bulk fluid composition, is now stated explicitly (l 121), which, I hope, also makes the transition to the lagged speciation section clear.

Reviewer 1 (Craig) asks for benchmarking/testing - I know the subduction zone calculations are meant to do this but perhaps you could take a simple system and illustrate how taking into account finite fluid solute compositions modifies the results - I sure there is room for this.

I have replaced Figure 1 with a modified version of what was Figure 2, and added simple quantitative phase diagram sections as Figure 2. I am grateful for the suggestion, which I believe does much to clarify a relatively opaque section.

Craig speculates on the conditiosn for algorithmic failure - if he is right this summary is a nice statement of the problem - you might think of incorporating it.

I have re-written the section 3.1 entirely, Craig’s statement summarizes a necessary, but not sufficient condition for algorithmic feasibility. A variant of his statement is incorporated in the revised Section 3.1 (last sentence of the first paragraph).

Reviewer 2 asks for comparison with other codes - my guess from reading your paper is why they don't work relates to mass balence with the fluid composition ie the the difference between say doing equlibrium calculations with a given set of minerals and calculating a pseudo-section?
Anyway a bit of explanation here might be useful.

See response to reviewer below.

I will leave it up to you how much revision you undertake but if the paper is as important as the reviewers claim it would be well worth making it as accessible as possible.

A few minor comments

1st sentence 'Back-calculated speciation designates the calculation of the solute speciation of an electrolytic fluid under the assumptions of charge balance, equilibrium, known solvent composition, and specified chemical potentials.

why not Back-calculated speciation calculates (or is used to calculate).

Changed to "The term ..." to emphasize this is a definition.

Fig 1 - explain colours and figure in caption.

This request led me to realize that I could not explain the figure and ultimately led me to replace Figures 1 and 2 and completely rewrite Section 3.1.

Harrison and Sverjensky, 2013) reference missing from supplementary material.

replaced by Sverjensky et al., 2014.

line 377 an 'at' missing.

corrected.

best wishes
mike

Reviewers' comments:

Reviewer #1: This is an extremely important contribution that deserves

publication with minor revisions. Integration of aqueous chemistry with petrologic computational approaches is a holy grail that is finally being realized. The present paper represents a major step forward. It builds on previous papers by Galvez et al, which showed the possibility and importance of integrating speciation calculations with petrologic minimization calculations. However, the Galvez contributions were less formally rigorous. Here, Connolly takes the methods to the next level by using an iterative energy minimization scheme. He applies the results to an important problem for illustrative purposes, and extracts useful insights while providing essential comparisons to previous results. In general, the paper is careful to highlight limitations and potential problems.

The discussion of the conditions for algorithmic failure is essential. However, it is worth emphasizing that the cases in which failure may occur could be pretty common. In particular, the first case is really important. There will be many instances in which an elementis present in the solution but not in a mineral; late in the discussion halogens are mentioned, but there are obviously more. To what extent is this mitigated by solid solution? Formally, any fluid solute must also be present in a mineral (or minerals) as well, as required by finite equilibrium constants for exchange equilibria with a relevant solid solution (albitic feldspar for the case of K, mica or amphibole for Cl, etc). Isnt the real problem not with lagged speciation but rather the family of solid solution models under consideration?

This section has been completely rewritten and, I believe, that all soluble components must be present among the stable solids is properly emphasized. While it is tempting to shift blame from the algorithm to solution models, I don’t think it’s fair. The practical reality is that solid solution models are incomplete. Moreover, the solubility issue is a necessary, but not sufficient, condition for algorithmic feasibility. In other words, the algorithm may fail even if all elements are soluble in all phases. However, I have added a statement (l 180) from which the reader may infer that more complex solution models may be helpful.

The second situation is also envisioned to be pretty common, but it seems like it is little more than the first problem but just for more than two components. For example, q+H2O+f is not a real assemblage, but isn't really just a consequence of the inability to put the additional component (CaO) in a mineral (wollastonite)? Obviously a difference here is that this issue can occur even in highly rock dominated conditions, near the q apex in figure 2.

The explanation of the second situation was not done well. The new explanation is not easy to follow, but it is logically complete. I hope that the implication of the limitation, that the probability of

failure increases toward the solid-saturation surface but is not known a priori, is clear. Few readers would benefit from a more elaborate explanation.

The exception Craig argues here is incorrect, or rather, he argues a case without defining what the rock-dominated limit means. The example has been clarified by the identification of the fluid- and solid-saturation surfaces in figure 1 (formerly figure 2). If the rock-dominated limit is defined as the fluid-saturation surface, the limit restricts to bulk compositions along the CaO-SiO2 join, where the stable assemblages may be in equilibrium with fluid but the amount of fluid is zero. This is not a particularly useful limit for natural systems, therefore in the text I argue that the limit is usefully defined as the conditions where the algorithm fails (l 245-250, as in the original text).

It might be worth noting that lagged speciation as formulated here is optimal not simply in the rock dominated case, but also in the many component case. Sort of like MELTS, which is useless for simple systems but powerful in compositional space well away from binaries and simple ternaries. That is, using Fig 2a as the example, not just near the wo-q join, but also away from the wo and q apices.

This is incorrect argumentation because it ignores the consequences of compositional degeneracy. Fig 2a illustrates a calculation in the simple binary SiO2-H2O. It is true that complexity does have a stabilizing influence, but that is essentially Craig's first point.

The transition from computational background to application is a big transition (lines 198-200). There is essentially no benchmarking or testing. While the real testing is the dataset against experiments, and thus not the responsibility of this paper, it would still be worth demonstrating that the new framework returns numbers that are identical to the dataset. Especially given that DEW is calibrated based on Berman 92 minerals rather than Holland and Powell. This could go in the appendix, and could serve in addition to confirm how little this choice of mineral data set actually matters.

I know that Craig has done both types of comparisons, but in my opinion such a comparison is only of interest if it shows that there is something wrong, in which case I would not attempt to publish the result.

I have verified implementation of the data against the DEW speadsheet calculator so I am confident the equation of state is correct. The program (Perple_X) outputs the partial molar Gibbs energies, molalities, activities, etc, so the interested user can verify that

the results correspond to an equilibrium and compare it to the output of other calculators.

It is true, that comparison of results calculated with EQ3 would be of some technical interest in that it would demonstrate that both programs converge to the same equilibrium from much different starting points. However, as solid solution models are implemented in EQ3 such convergence would hardly be surprising.

I have added a comparison (Figure A.1) that illustrates the effect of the condensed phase thermodynamic data (i.e., Holland vs Berman) to the appendix. As Craig anticipates, and likely knew in advance, it is uninteresting.

The DEW model is stated be applicable only to 6 GPa. Extension to higher pressures needs to be discussed, presumably best done in appendix.

There is not much to discuss, most of the solute data is based on primitive linear correlations, and the dielectric constant is roughly a measure of solvent density. As the solvent density varies smoothly with pressure and temperature, it is not implausible to expect the model can be extrapolated. This point is now made in the appendix.

Minor tweaks:
Line 16: subducted not subduction

corrected

19: why "putative"?

because the extent of the slab serpentinization is not established and, I personally, am doubtful that it generates a pervasive flux through the crust. My reasons for “putative” are elaborated in final paragraphs of the “conclusion” (formerly the end of the discussion).

34: omit "Galvez et al"

corrected

79: consider adding citation to Galvez et al or adding a topic sentence to improve clarity. It is not immediately obvious that the purpose of this section is to compare/contrast back calculation to lagged speciation. But obviously one figures it out eventually

Citation added, the intent of the section is/was specified in the previous paragraph.

85. …amount of component j in i and…

the list was/is preceded by "for species i:"

93. I am probably missing something but seems like the ratio of charges should be q(i)/q(k), not q(k)/q(i)

Corrected.

98. …T is absolute temperature…

Changed.

111-112: Regardless of the details of the back-calculation method, it is inexact. If the solvent…

Changed, but "flaw" retained. Inexact is ambiguous, the method may be an excellent approximation, the problem is that the method is inconsistent with its assumptions and, in essence, this introduces a path dependence to the result.

140-144: Will this be important for mass balance of important species present as both solvent components and ionic solutes, e.g., carbon and sulfur? Would be worth minor elaboration

Unchanged. Any inconsistency in the activity models is potentially important, but evaluating the importance requires a consistent model for comparison. Consistent models are available for some simple chemical systems. The intent here is to treat chemically complex systems where, at present, no formulation exists that is both practical and consistent. The present treatment is in any case better than the common practice of assuming solvent species activities are independent of solute chemistry.

152: result, convergence (add comma)

Corrected.

163: no "a" in figure 1, line is purple not blue

The figure has been deleted. i would argue the color was blue, but to avoid any ambiguity i have changed the "blue" to what is technically in "cyan" in the new figures 1 and 2.

186: iterations there ARE from the algorithmic perspective

Corrected.

189: system's

Reworded to avoid the possessive for an inanimate object.

191: something is missing. The examples don't illustrate the rock dominated limit, but rather with the need to work near that limit, or whatever.

Reworded as "problems that arise beyond the rock-dominated limit"

195: Gibbs energy minimization procedure is

Corrected.

204: lithologies are heterogeneous; rather than (semi colon not comma)

Corrected.

200-210: GLOSS has been updated by Plank (2013). Syracuse et al (2010) is almost universally used to compare and contrast subduction geotherms. Is there a reason to avoid these more recent works?

I was under the mistaken impression that GLOSS and GLOSS-II had the same major element chemistry. They do not, but they do not differ within the stated error; therefore, to avoid the unpleasantness of redrafting the figures I have retained GLOSS.

Syracuse et al. (2010) is a set of geotherms for ~50 subduction zones computed by the same method, and the same quality of input data, as used by Ruepke et al. (2004). They do not identify a representative global model, thus there is no reason to prefer the work. The text now observes (Section 4.1, final paragraph) that the Ruepke geotherm is at the cool end of the Syracuse et al. spectrum. As such, the Ruepke geotherm represents a best case scenario for sub-arc C dissolution.

243: …only the four dominant solvent-molecule species…

Corrected.

247: …and to inform understanding of the devolatilization process.

Corrected. I guess "inform understanding of" is less pompous than to understand.

313: …during subduction, such models…

Corrected.

317-318: this is because almost all Al is in polymerized species for which there are no current thermodynamic data (Manning 2007, 2010, 2018 Annual reviews of earth and planetary sciences).

This point was made in the discussion. Manning (2007, 2010) cited there are now repeated at this location.

337: …solvent model does not… (no comma)

Corrected.

378: …the slab at pressures…

No change. "...the slab is at pressures..." seems correct to me.

--Craig Manning

Reviewer #2:

This manuscript consists of two parts that are not really tightly related to each other. One part describes a back-calculation "lagged speciation" approach to compute aqueous speciation in equilibrium with a rock mineral assemblage in a wide range of temperature and pressure conditions (section 2) and its algorithmic limitations (Section 3). Another part is devoted to petrological analysis of large-scale decarbonatisation and K-depletion processes in subduction zones with some inferences on CO2 mass fluxes into the upper Earth crust from subducted lithospheric slabs. The discussion topics and conclusions

formulated by the author are subject to scientific discussion and cannot be praised or criticised in the context of criteria of acceptance for publication. In fact, the level of this paper, technical details and data, quality of figures, logics of the discussion and English style are all high enough for a publication aimed at triggering and/or contributing to
discussion of CO2 fluxes and fate in the global tectonically-driven turnover of the Earth crust.

It's not clear to me where the reviewer is heading with these comments. He doesn't seem particularly happy with paper as it is (and I can see his point) yet his final sentence seems to be an endorsement. He is correct that the application is not tightly tied to the presentation of the algorithm and it worries me that it will be lost as a consequence. But the loss will be, I hope, mine rather than the reader's.

There is one aspect of the first (methodical) part of the manuscript that needs commenting and elaboration. The author describes the "lagged speciation" algorithm (a generalization of their earlier "back-calculation" method) in which the calculation of equilibrium speciation begins with the system involving all solid phases and the aqueous fluid without solutes. Then the amounts of solutes are estimated and added to the mass balance at the next stage, repeated until convergence. For rock-dominated systems, this non-rigorous scheme mirrors the one used in LMA algorithms (MINEQL, PHREEQC, CHILLER, etc.) for water-dominated systems, where the initial calculation of equilibrium speciation is performed without including minerals to the mass balance, then the saturation indices are estimated for all minerals, and the most oversaturated one is added to mass balance, the hole process repeated until no oversaturated minerals are left in the list. As discussed in (Leal et al. 2017), canonical Gibbs energy minimization GEM methods do not require such non-rigorous iterative procedures because they can solve the complete heterogeneous equilibrium state in one run, even without a good initial guess (in this case a Simplex feasible initial guess is automatically obtained). GEM codes (e.g. ThermoCalc, FactSage, GEMS, HCh), some available open-source, could be used in calculations pertinent for the second part of the title manuscript.

This statement is exactly the difficulty I described in my original cover-letter. The reviewer is technically correct, but the operative word in his statement is "could". ThermoCalc and FactSage are commercial variants of one of the first optimization codes (SOLGASMIX). There is no question that the commercial versions of SOLGASMIX can handle the kinds of order-disorder models that are now common in petrology. However, these codes are applied to simple

chemical systems and, so far as I am aware, it remains to be demonstrated that they perform as well in complex chemical systems. Aside from the commercial aspect of these codes, they do not implement petrological models or, for that matter, models for high pressure aqueous solutes. HCh is a commercial black box, but is targeted at earth science applications. I can find no publication that suggests it has the capacity or to treat petrological models. Of the codes listed by the reviewer only GEMS is open source. Five years ago I was asked by people working on GEMS for assistance in implementing petrological order-disorder models. At the conclusion of that episode I was told that order-disorder models could not be implemented. I am inclined to believe that failure reflected competence rather than any algorithmic limitation. However, regardless of that possibility, I can find no evidence from recent publications that such models or, for that matter, the DEW solute model/data, have been implemented in GEMS.

When reading it, the reader becomes progressively unsure why the author used the "lagged speciation back calculation" procedure in favour of rigorous GEM codes. Also, no benchmarks with GEM codes were described that would show pros and cons of both groups of methods. If the argument was to extend the Perplex code family with aqueous equilibria, this could be discussed more explicitly.

In fact, I have done my best to make the reader unsure. My hope is that that insecurity will encourage the reader to examine and compare alternative possibilities. Because of the practical limitations I mention above, benchmarks would require the presentation of calculations in simplified model systems of little petrological interest. Given the limits on paper length and, more importantly, the patience of the readership I prefer to use that aliquot of patience on a petrologically relevant problem.

Overall, my recommendation to the author, who is one of the most respected experts in his field, is to undertake a minor revision where to
summarise the arguments in favour of his choice of computational methods and tools in the context of comparison with LMA and canonical GEM methods and the Perplex (discretisation +Simplex method- based algorithm). This would reduce possible confusion for the reader, and increase the impact of this interesting paper.

The anonymous reviewer has a much better understanding of optimization methods than I do and I do not question the legitimacy of any of the

issues that he raises. However, his suggestion that I contrast lagged-speciation with other algorithms again raises the dilemma I mentioned in my original cover letter. To wit, there is no disputing there are superior algorithms, and that these are implemented in various codes, but these codes do not necessarily have superior practical capabilities. For the great majority of the EPSL readership the issue of importance is not whether a code is based on a superior algorithm, rather it is the capabilities of the code. Therefore I disagree with the reviewer's opinion that a discussion of algorithms would enhance the impact of the paper. To the contrary, I believe such a discussion is likely to repel readers. To ease my conscience about only mentioning robust algorithms in the discussion, I have added a sentence at the end of the opening paragraph to alert the reader (the Karpov et al. reference is the basis for GEMS).

***Highlights (for review)**

Highlights:

- Electrolytic fluid speciation is implemented in a Gibbs energy minimization code.
- Dissolution increases C-solubility two-fold compared to molecular fluid models.
- Infiltration-driven decarbonation desiccates the crust by K-depletion.
- Sulfides become soluble by the reduction of carbonate to diamond at ~6 GPa.

Electrolytic Fluid Speciation by Gibbs Energy Minimization and Implications for Subduction Zone Mass Transfer

James A. D. Connolly and Matthieu E. Galvez
Department of Earth Sciences
Swiss Federal Institute of Technology
CH-8092 Zurich

E-mail address: james.connolly@erdw.ethz.ch

Abstract

The number of solute species required to describe the thermodynamic behavior of electrolytic fluids is a hindrance to the incorporation of aqueous geochemistry in petrological Gibbs energy minimization procedures. An algorithm is developed to overcome this problem. Beginning from the solute-free limit, chemical potentials, and phase stability are determined by minimization, the solute speciation and bulk fluid properties consistent with these chemical potentials are then computed and the procedure repeated until the chemical potentials converge. Application of the algorithm to a model for metamorphism of subducted sediment shows that accounting for solute chemistry does not change the conclusion based on molecular fluid models that a pervasive water flux from the subjacent mantle is required to explain island-arc carbon emissions by fluid-mediated slab decarbonation. This putative flux would deplete the sediment in potassium, limiting the capacity of the slab to transport water to greater depth and rendering it refractory to melting.

Keywords: Electrolytic fluid speciation, Gibbs energy minimization, subduction, devolatilization, mass transfer, decarbonation.

1. Introduction

Gibbs energy minimization is applied to a broad spectrum of geochemical and petrological problems (Leal et al., 2017). In geochemistry the focus of these applications is usually modelling reactive transport (Wolery, 1992; Bethke, 1996), whereas in petrology the focus is predicting phase stability (DeCapitani and Brown, 1987; Connolly, 2009). This disparity has led to a situation in which many geochemical codes account for complex fluid chemistry, but seek only a local equilibrium solution, whereas petrologic codes seek a costly global solution that limits their ability to treat the complex fluid chemistry. As a means of bridging this gap Galvez et al. (2015; 2016) use phase equilibria computed by Gibbs energy minimization assuming a solute-free fluid to back-calculate solute chemistry. This method accurately estimates solute chemistry provided the solute mass is small compared to the total mass of the system, but is not well suited for reactive transport problems because the phase proportions and bulk fluid chemistry are not rigorously determined. The present work improves on this method by incorporating back-calculated fluid chemistry in an iterative Gibbs energy minimization procedure referred to here as lagged speciation. It should be remarked that there are completely robust geochemical codes (Harvie et al., 1987; Karpov et al., 2001), which, at least in principle, are capable of treating petrological models.

The utility of the lagged speciation algorithm is demonstrated by a model for devolatilization of subduction zone sediments. This problem has been made tractable by the Deep Earth Water (DEW) model for electrolytic fluids (Sverjensky et al., 2014), which extends the Helgeson-Kirkham-Flowers (HKF) formulation (Shock et al., 1992) for aqueous species to high pressure conditions. Although a number of studies have considered the implications of the DEW model for fluid-dominated subduction zone chemistry (Facq et al., 2014; Sverjensky and Huang, 2015;

Tumiati et al., 2017), the present focus is the rock-dominated limit appropriate in systems where the fluid is generated by devolatilization. This limit was investigated by Galvez et al. (2015) using a variant of the DEW model. The distinction between the DEW model and the Galvez et al. (2015) variant, is that in the DEW model the solvent is H_2O and molecular volatiles are treated as solute species, whereas in Galvez et al. (2015) the solvent is a mixture of molecular volatiles. Both approaches are compared.

Subduction zone devolatilization is topical because of its potential role in various global element cycles. The observation, based on simple sub-solidus phase equilibrium models (Kerrick and Connolly, 2001ab) that carbonates persist within subducted slabs beyond sub-arc depth has motivated alternative hypotheses to explain extensive slab decarbonation. These hypotheses include: infiltration-driven decarbonation (Connolly, 2005; Gorman et al., 2006); C transfer by entrainment or diapirism (Dasgupta et al., 2004; Behn et al., 2011); slab-melting (Poli, 2015; Skora et al., 2015); or near-surface provenance volcanic CO_2 (Mason et al., 2017). With the exception of the latter, all of these mechanisms are viable but unsatisfying in that they require a coincidence of processes or extreme temperatures. Evidence of sub-solidus carbonate dissolution (Frezzotti et al., 2011; Ague and Nicolescu, 2014) has prompted the suggestion that, by neglecting the solubility of non-volatile elements, early models underestimated the efficacy of simple decarbonation processes. Previous work (Kelemen and Manning 2015) indicates dissolution may cause a two-fold increase in the carbon-content of subduction zone fluids, but does not address fluid production. The models here extend that work by tracking fluid evolution from the surface to beyond sub-arc depths.

This paper begins with a generalization of the back-calculation method (Galvez et al., 2015). The lagged speciation algorithm by which back-calculated results may be integrated into a Gibbs energy minimization procedure is then outlined and the limitations of the algorithm are

explained. The final major section uses the subduction zone model to illustrate some technicalities of the method and to explore the consequences of solute chemistry on closed, open, and infiltration-driven devolatilization scenarios.

2. Back-Calculated Speciation

The term back-calculated speciation designates the calculation of the solute speciation of an electrolytic fluid under the assumptions of charge balance, equilibrium, known solvent composition, and specified chemical potentials (Galvez et al., 2015). The partial molar Gibbs energy of any species can be expressed as

$$g^i = -n^i_{e-}\mu_{e-} + \sum_{j=1}^{c} n^i_j \mu_j \qquad 1$$

where c is the number of components, μ_j and μ_{e-} are, respectively, the chemical potential of component j and the electron, and for species i: n^i_j is the molar amount of component j, and $-n^i_{e-}$ is the molar charge, abbreviated hereafter q^i. Equation 1 can be rearranged to express μ_{e-} in terms of the chemical potentials and the properties of charged species i

$$\mu_{e-} = \frac{1}{q^i}\left(g^i - \sum_{j=1}^{c} n^i_j \mu_j\right). \qquad 2$$

Because μ_{e-} is the same for all species at equilibrium, the partial molar Gibbs energy of any arbitrarily chosen charged species (g^i) can be related to the partial molar Gibbs energy of a charged reference species (g^k) by equating the right-hand-side of Equation 2 for both species

$$\frac{1}{q^i}\left(g^i - \sum_{j=1}^{c} n^i_j \mu_j\right) = \frac{1}{q^k}\left(g^k - \sum_{j=1}^{c} n^k_j \mu_j\right). \qquad 3$$

Rearranging Equation 3, the partial molar Gibbs energies of any charged species can then be expressed in terms of the reference species partial molar Gibbs energy and the chemical potentials of the system

$$g^i = \frac{q^i}{q^k}\left(g^k + \sum_{j=1}^{c} \mu_j \Delta n_j^i\right) \qquad 4$$

where $\Delta n_j^i = n_j^k - n_j^i$. In terms of a solute reference state activity model, the partial molar Gibbs energies in Equation 4 are

$$g^i = g^{*,i} + \mathrm{R}T \ln\left(m^i \gamma^i\right) \qquad 5$$

where $g^{*,i}$ is the solute reference state molar Gibbs energy, m^i is the molal concentration, γ^i is the activity coefficient, T is absolute temperature, and R is the universal gas constant. Applying Equation 5 in Equation 4 and rearranging the result

$$m^i = \frac{c^i}{\gamma^i}\left(m^k \gamma^k\right)^{q^i/q^k} \qquad 6$$

where

$$c^i = \exp\left(\frac{q^i}{q^k}\left[g^{*,k} + \sum_{j=1}^{c} \mu_j \Delta n_j^i\right] - g^{*,i} \Big/ \mathrm{R}T\right).$$

Substituting Equation 6 into the charge balance constraint for a fluid with s charged solute species

$$\sum_{i=1}^{s} q^i m^i = 0 \qquad 7$$

yields

$$\sum_{i=1}^{s} \frac{q^i c^i}{\gamma^i}\left(m^k \gamma^k\right)^{q^i/q^k} = 0\,, \qquad 8$$

which can be solved in the ideal limit ($\gamma^i \rightarrow 1$) for m^k if the composition of the solvent, which influences $g^{*,i}$, is known. The concentrations of the remaining charged species are then obtained from Equation 6 and those of neutral species from Equation 5.

In the non-ideal case, additional assumptions are necessary to compute the activity coefficients in Equations 5, 6, and 8. Regardless of those assumptions, the method is flawed: if the solvent

composition is consistent with the specified chemical potentials, as is the case when the chemical potentials and solvent composition are obtained by Gibbs energy minimization, then finite solute concentrations violate this consistency. This flaw has the consequence that, except in the limit of infinite dilution ($m^i \rightarrow 0$), there is no bulk fluid composition that simultaneously satisfies Equation 8 and the constraint on the chemical potentials of the system, i.e., there is no thermodynamically robust relation between fluid speciation and bulk composition.

3. The Lagged Speciation Algorithm

The limitation of simple back-calculated speciation is the absence of a relation between the calculated solute chemistry and the bulk chemistry of the fluid, which precludes evaluation of mass balance constraints. To circumvent this limitation, the present work exploits the iterative aspect of Gibbs energy minimization by successive linear programming (Connolly 2009). The essential feature of successive linear programming is that an initial result in which the compositions of the phases are discretized at some specified resolution is iteratively refined until a desired target resolution has been achieved. The innovation here is to use a minor modification of the back-calculated speciation algorithm to estimate the Gibbs energy and composition of the stable fluid(s). In the initial optimization, the fluid may contain multiple solvent species (e.g., H_2O, CO_2, CH_4, H_2S), but is solute-free. Given the solute-free solvent composition(s) and chemical potentials obtained in this optimization, the reference state solute partial molar Gibbs energies are computed, Equation 8 is solved for the concentration of the reference ion, and Equations 5 and 6 are solved for the concentrations of the remaining solute species. The solvent mole fractions are then recomputed as

$$y^i_{h+1} = \frac{m^i_h}{m_{total}} \quad i = t+1,\ldots,r \qquad 9$$

with

$$m_{total} = \sum_{i=1}^{t} m_h^i + \sum_{i=t+1}^{t+r} y_h^i \qquad 10$$

where t is the total (charged + neutral) number of solute species, r is the number of solvent species, and h indexes the iteration level. The specific Gibbs energy and bulk composition for the fluid used in the succeeding iteration are

$$g_{h+1} = \sum_{i=1}^{t} \left(m_h^i \left[g^{*,i} + \mathrm{R}T \ln\left(m_h^i \gamma_h^i \right) \right] \right) + \sum_{i=t+1}^{t+r} \left(m_h^i \left[g^{0,i} + \mathrm{R}T \ln\left(y_{h+1}^i \gamma_{0,h}^i \right) \right] \right) \qquad 11$$

$$n_{j,h+1} = \sum_{i=1}^{t} m_h^i n_j^i + \sum_{i=t+1}^{t+r} m_{h+1}^i n_j^i \quad j = 1, \ldots, c\,, \qquad 12$$

where $\gamma_{0,h}^i$ is the activity coefficient of solvent species i in the solute-free solvent. Equation 11 ignores the dependence of the solvent species activity coefficients on solute concentration and is therefore thermodynamically consistent only in the ideal limit (e.g., Wolery 1990). Although it is not algorithmically required, the inconsistent form is maintained because electrolytic fluid species activity models are currently poorly constrained. In contrast, molecular fluid equations of state are capable of predicting species activities in the solute-free solvent with good accuracy (Prausnitz, 1969). Excepting this inconsistency, and in contrast to simple back-calculation, iterative application of Equations 11 and 12 reaches a thermodynamically consistent solution provided the lagged chemical potentials, used to compute the solute molalities m_h^i by back-calculation, converge.

To distinguish back-calculation during lagged speciation from simple back-calculation (Galvez at al., 2015), simple back-calculation is defined as the solute species concentrations and fluid bulk compositions m_0^i and $n_{j,1}$, respectively, in Equation 12.

3.1 Algorithmic Limitations

The chemical potentials of all soluble components of a system are necessary to back-calculate fluid speciation. It follows that a necessary condition for algorithmic feasibility is that any component represented in the fluid only by solute species must be present in at least one phase other than the fluid. The nature of this limitation is illustrated schematically (Fig 1) for the CaO-SiO_2-H_2O system under conditions such that stoichiometric lime (lm; see Table 1 for phase notation), wollastonite (wo), and quartz (q) are stable solids and the solvent is considered to consist only of H_2O. In simple back-calculation, the chemical potentials of all components are computed for the solute-free system (Fig 1a). Thus, for any general bulk composition, the chemical potentials correspond to those of the assemblage lm + wo + water or wo + q + water. Each of these assemblages yields a fluid (F) composition that may be iteratively refined by lagged speciation to yield a point on the fluid-saturation surface of the system. In the course of this refinement, the lm + wo + F and wo + q + F phase fields shrink creating phase fields with finite area for lm + F, q + F, and F (Fig 1b). The soluble components SiO_2 and CaO are not present in, respectively, lm and q. Therefore, the lagged speciation algorithm becomes infeasible during iteration for bulk compositions that lie within the lm + F, q + F, and F phase fields. A consequence of this limitation is that the treatment of elements of geochemical interest, such as Cl, U, and Au, is only possible if a solid host for the element is stable.

The presence of the soluble components in the stable solid phases of a system is a necessary, but not sufficient condition, for algorithmic feasibility. The sufficient condition relates to the manner in which chemical potentials are determined from the linearized formulation of the Gibbs energy minimization problem (Connolly, 2009). This relationship is not easily explained, so it may be helpful to note that the most important manifestation of the sufficient condition is that the lagged speciation fails if the number of compositional degrees of freedom associated with the

fluid phase increases during iteration. Thus, the lagged speciation will fail for any bulk composition that lies within the two-phase fields of the CaO-SiO_2-H_2O phase diagram (Fig 1b) and, in phase diagram sections as a function of pressure and temperature, the failure condition usually coincides with a phase boundary across which the number of solid phases decreases.

In painful detail, the origin of the sufficient condition is that in successive linear programming the possible compositional variation of any phase is discretized, and the discrete states are treated as individual phases in the internal representation of the problem. Consequently, any stable phase assemblage is represented internally as an invariant assemblage consisting of as many discrete states as the system has components. If the true variance of the phase assemblage is greater than zero, then the internal representation must include more than one discrete composition of a stable phase. These internal phases are homogenized to form the true phases of the final result. The maximum number of internal phases that may represent a single true phase is equal to the number of independently variable components in the phase (Connolly, 2009). In the case of back-calculated speciation, soluble components in the fluid phase are not independently variable because they are determined by the coexisting solids; therefore, the maximum number of internal phases that may represent the fluid in any given assemblage is equal to the number of solvent components. In the CaO-SiO_2-H_2O example, as the solids possess no compositional degrees of freedom and the solvent has only one component, it is impossible to represent a phase assemblage of $< c = 3$ phases. Thus, lagged speciation becomes infeasible during iteration for bulk compositions that lie within the wo + F phase field even though both solute components are present in wo.

The CaO-SiO_2-H_2O example is potentially misleading in that the relationship between feasibility and variance is specific to the case illustrated. There is no such relationship in general. However, because any stable phase assemblage is represented internally by an invariant set of

discrete phase states, the example illustrates a general relationship between the bulk composition and the solid- and fluid-saturation surfaces. Specifically, that the probability of specifying an infeasible bulk composition approaches zero in the limit that the bulk composition nears the fluid-saturation surface and approaches unity in the limit that the bulk composition nears the solid-saturation surface.

Two calculations illustrate the manifestation of infeasibility conditions quantitatively (Fig 2, see the Appendix for thermodynamic details). For a system composed of 1 kg H_2O + 10 mol SiO_2 (Fig 2a) the infeasibility conditions map the solid-saturation surface as a function of pressure and temperature. The maximum in Si-solubility at high pressure and intermediate temperature reflects the dominance of ionic species ($HSiO_3^-$) at low temperature and molecular species (SiO_2, Si_2O_4) at high temperature (Manning, 2010; Sverjensky et al., 2014). The change in solubility mechanism has the consequence that the high-temperature solid-saturation surface coincides with the 1 molal Si-isopleth for the fluid, whereas the low temperature solid-saturation surface lies at slightly higher Si-molality because the formation of H-bearing solute species reduces the solvent mass (H_2O). The system composed of 20 mol H_2O + 12 mol SiO_2 + 0.5 mol K_2O + 1 mol Al_2O_3 (Fig 2b) illustrates a case where the necessary condition for feasibility is insufficient, in that all soluble components are present in the stable solids at the limit of the feasible conditions. In this example, the limit of feasible conditions coincides with the low pressure boundary of the mu + q + F phase field, analogous to the wo + F field in the schematic CaO-SiO_2-H_2O example (Fig 1b). That lagged speciation is feasible in the high-variance melt phase fields (Mlt + q + F and Mlt + F) demonstrates that the sufficient condition for feasibility is not directly related to phase field variance. Both examples demonstrate that even in relatively fluid-rich systems, simple back-calculation may provide accurate solubility estimates and therefore that the chief benefit of lagged speciation is that it automatically defines phase changes caused by solubility.

Although the necessary condition for feasibility is redundant in light of the sufficient condition, the necessary condition has been discussed because its chemical significance is evident. The conditions for algorithmic feasibility illustrate problems that arise in fluid-rich systems and raises the question of whether the rock-dominated limit of Galvez et al. (2015) can be usefully defined. From a phase equilibrium perspective, the only robust formulation of this limit identifies it as the fluid-saturation surface, i.e., the conditions at which fluid is stable, but its amount is zero. As such the limit is unduly restrictive and has no practical utility other than to indicate that back-calculation is likely to be accurate if the fluid mass is small. An alternative formulation of the rock-dominated limit adopted here is that it corresponds to the conditions at which lagged speciation becomes infeasible. Within this limit the lagged speciation is unconditionally stable.

4. Devolatilization of Subduction Zone Sediment

To provide a minimal model for subduction zone devolatilization the geotherm (Fig 3) adopted here represents subduction of a young (40 Ma) slab at a rate of 10 cm/y and a kinematically prescribed dip of 45° (Rupke et al., 2004). Comparison to the compilation of Syracuse et al. (2010) suggests that the model sub-arc temperatures are close to the lower limit of plausible subduction zone conditions. As such, the model maximizes the importance of electrolytic solutes. Sediment lithologies are heterogeneous; rather than consider this compositional spectrum, the global average marine sediment (GLOSS; Plank and Langmuir, 1998) composition is taken to be representative (Table 2). Previous phase equilibrium modeling (Kerrick and Connolly, 2001a) indicates that the high GLOSS water-content favors decarbonation at low temperature compared to water-poor carbonate sediments and as such provides a best case scenario for sub-arc decarbonation. Because the GLOSS average does not quantify the redox state of iron or carbon, the initial bulk oxygen content is computed under the assumption that all iron is ferrous and all carbon is present as carbonate, a configuration

identified here as the neutral bulk redox state. In the resulting models, the stability of ferric iron in low-temperature minerals has the consequence that a small amount of carbonate is reduced to form graphite at surface conditions and graphite or diamond persists, except in the infiltration model, as a stable phase at all conditions. Preliminary calculations demonstrated that an implausible initial ferric/ferrous ratio of ~2.5 would be necessary to completely suppress the stability of reduced carbon during devolatilization. At the opposite extreme, essentially all the initial carbon must be reduced to destabilize carbonate. This extreme leads to dramatically different devolatilization behavior in that at low pressures (< ~1.5 GPa) almost all carbon is released in the form of a methane-rich fluid, an effect that may be of some interest but effectively eliminates decarbonation as a mechanism for explaining island-arc carbon emissions. These considerations suggest that predictions based on the neutral bulk redox state initial condition are likely to be characteristic of natural conditions and, to a first approximation, account for the presence of organic carbon in marine sediments (Bebout, 1995).

Sulfur is an important, but oft neglected, component of subduction zone volatile budgets (Pokrovski and Dubrovinsky, 2011; Evans et al., 2014; Kagoshima et al., 2015; Canil and Fellows, 2017). To evaluate the effect of Sulfur, the GLOSS composition (Table 2) was modified by the addition of 0.1 mol S_2/kg. The sulfur is presumed to be accommodated in pyrite (~0.6 vol %) and the bulk oxygen content reduced accordingly, i.e., the bulk molar O_2 content is reduced by half the molar S_2 content. The possibility of the presence of oxidized sulfur in the initial bulk composition was not considered because in preliminary calculations sulfates were not predicted to coexist with graphite + carbonate at surface conditions.

The HKF/DEW data base (Shock et al., 1992; Sverjensky et al., 2014) includes 28 C-O-H-S solute species. In initial calculations the concentrations of glycolate ($C_2H_3O_3^-$), glutarate ($C_5H_7O_4^-$), and lactate ($C_3H_5O_3^-$) were implausibly high at all conditions of interest. Accordingly,

these species were not considered in the H_2O-solvent model calculations. In mixed-volatile solvent calculations (the COHS-solvent model), none of the HKF/DEW C-O-H-S organic and/or molecular solute species were considered, and the solvent was initially treated as a mixture of H_2O, H_2, CO, CO_2, CH_4, SO_2, and H_2S species. These calculations demonstrated that H_2, CO, CH_4, and SO_2 had no significant effect on solute speciation or bulk chemistry. The final calculations considered only the four dominant solvent species (H_2O, CO_2, CH_4, and H_2S).

Results are presented for closed system sediment devolatilization computed by lagged speciation with the COHS-solvent model. These results are compared to four variants to illustrate technical differences and to inform understanding of the devolatilization process. Specifically, the variants, and their purposes, are: 1) simple back-calculation, to contrast the lagged- and back-calculation methods; 2) H_2O-solvent, to illustrate the consequences of the choice of solvent model on fluid speciation and chemistry; 3) fluid-fractionation, a more realistic open-system model for devolatilization; and 4) infiltration-driven devolatilization, an effective, if poorly constrained, mechanism for slab-decarbonation.

Thermodynamic details of the model calculations and the implementation of the HKF/DEW formulation are summarized in the Appendix. The computer program and data files used for these calculations are available at www.perplex.ethz.ch.

4.1 Devolatilization vs Dissolution

The difference between the phase proportions predicted for GLOSS subduction models that account for both devolatilization and dissolution (Fig 4a) and a model without dissolution (Fig 4b) is surprisingly large. Most notably in the absence of dissolution white mica undergoes no significant dehydration. In contrast, in the lagged speciation model, mica is almost completely dehydrated at the maximum pressure, 6.6 GPa, of the profile. Likewise, without dissolution, the

proportions of pyrite and aragonite are approximately constant after dolomite is destabilized at ~5 GPa, but in the lagged speciation model pyrite and aragonite are eliminated by dissolution at 6.4 GPa. The maximum pressure at which phase relations are computed in the lagged-speciation calculation is the point at which the fluid composition becomes so solute-rich that the rock-dominated limit (Fig 2) is violated.

Although not easily visible (Fig 4b), the volume of diamond increases ten-fold, to ~0.1%, over the same interval that aragonite begins to dissolve. From the fluid speciation (Fig 5a), it is apparent that this phase of diamond precipitation is related to an increase in the concentration of $CaSO_4$ in the fluid, which forms by the reduction of carbon bound in aragonite. This prediction is consistent with the observation of sulfate species and solid carbonate in fluid inclusions in natural subduction zone diamonds (Frezzotti et al., 2011). In calculations not reproduced here, Aragonite and mica are destabilized at essentially the same conditions for the S-free GLOSS composition; therefore, this process is not dependent on the stability of aqueous $CaSO_4$ and the oxidation of pyrite.

As anticipated by earlier studies (Manning et al., 2013; Galvez et al., 2015), dissolution roughly doubles carbon-loss during relatively cool subduction (Fig 6a) . In early models of slab-decarbonation (Kerrick and Connolly, 2001ab), closed-system results were used to estimate carbon-transfer under the assumption that the accumulated fluid is released in a single batch at sub-arc depth. On a global scale the fluid-mediated mass transfer of element *i* is

$$Q_i = v_s h_0 \rho_0 N_i n_i \qquad 13$$

where v_s is the global subduction rate (2.7 km^2/y; Plank and Langmuir, 1989), h_0 and ρ_0 are initial thickness and density of the source rock, N_i is the atomic weight, and n_i is the number of moles of element released by a unit mass of the source rock (Fig 6a). For present purposes, it is

assumed that the bulk of the slab carbon is contained in a 1300 m thick section consisting of 800 m of GLOSS sediment (Plank and Langmuir, 1998) and 500 m of hydrothermally altered basalt (Staudigel et al., 1989). Both lithologies have comparable initial carbon-content (0.7 mol/kg) and density (2600±100 kg/m^3) in which case the carbon input by subduction of oceanic crust is 76 Mt/y, which lies within the range of recent estimates (35-88 Mt/y; Kerrick and Connolly, 2001a; Dasgupta and Hirschmann, 2010; Kelemen and Manning, 2015). To make a first order assessment of the global carbon-loss, it is assumed that carbon-loss in the basalt section is comparable to that computed for GLOSS sediment. Justification for this assumption follows from the mineralogical similarity of sedimentary and basaltic eclogites (Kelemen and Manning, 2015). Based on these assumptions the global carbon-loss for batch devolatilization with (n_C = 0.28 mol/kg, Fig 6a) and without (n_C = 0.12 mol/kg) dissolution is, respectively, 30.6 Mt/y and 13.1 Mt/y, these values compare with estimates of island-arc carbon emissions (18-55 Mt/y; Kerrick and Connolly, 2001a; Dasgupta and Hirschmann, 2010; Kelemen and Manning, 2015). At face value, this result suggests dissolution resolves the mismatch between carbon loss predicted by the closed-system model and observed carbon emission. That conclusion is not justified in light of model uncertainty. Typical sub-arc temperatures may exceed those estimated here by ~100 K (Syracuse et al., 2010). Such an increase in sub-arc temperature would increase molecular CO_2 solubility five-fold (Connolly, 2005). While electrolytic chemistry would moderate this increase it is likely that such thermal effects dwarf the effect of dissolution (Galvez et al., 2016). Thus the criticism that closed-system devolatilization models are incapable of explaining island-arc carbon emissions is misplaced. The legitimate criticism of closed-system models for assessing carbon-loss is that the implied batch mechanism for fluid release is physically implausible.

Although the closed-system model does not provide a realistic basis for assessment of slab-mantle mass transfer during subduction, such models generally provide an upper limit for mass

transfer effected without the infiltration of externally derived fluids (Kerrick and Connolly, 2001b). As such, the closed-system model suggests that devolatilization processes have the potential to deplete K, H and S from subducted sediments, and almost no capacity to effect Fe or Al mass transfer. The immobility of Al is at odds with experimental observation (e.g., Tsay et al., 2017) and may merely reflect the current limitations of the solute-species model (Manning, 2007; Manning et al., 2010).

4.2 Simple Back-Calculated vs Lagged Speciation

Simple back-calculated speciation (Galvez et al., 2015) assumes the mineralogy and solvent chemistry obtained by a solute-free phase equilibrium model (e.g., Fig 4b), as such the simple back-calculated model cannot account for the effects of dissolution on mineral stability. However, it is appropriate to compare the lagged and back-calculated fluid speciation to assess the accuracy of back-calculation as an approximation of fluid chemistry. This comparison (Fig 5a) is reassuring in that, at conditions within the rock-dominated regime (i.e., pressure < 6.7 GPa), the simple back-calculated speciation is generally accurate to within a factor of two or better. Thus, the only prominent disadvantage of simple back-calculation is that it provides no means of recognizing the conditions at which the assumption of a rock-dominated regime is invalid.

4.3 H2O- vs COHS-Solvent

Comparison of phase equilibria computed for the H_2O- and COHS-solvent models (Fig 4a, Fig 5b, Fig 6b) reveals only minor differences. Both models predict CO_2 as the only major C-O-H-S species (Fig 5b). Of the 25 C-O-H-S solute species considered in the H_2O-solvent model, but excluded from the COHS-solvent model, only formate ($HCOO^{2-}$) is predicted to be stable at concentrations in excess of 10^{-2} m, a prediction consistent with the observation of abiotic formate as a prominent species in sea-floor hydrothermal systems (Lang et al., 2018). Although no molecular C-O-H-S solute species were included in the COHS-solvent calculation, the use of

a mixed-volatile solvent model does not preclude the simultaneous treatment of molecular volatile solute species.

From a computational perspective the advantage of the H_2O-solvent model is that it is inexpensive and accurate in the limit of dilute molecular solute concentrations. The chief disadvantage of the model is that it cannot be used predict phase separation, for example, the coexistence of H_2O- and CH_4- or CO_2-rich fluids (Fruh-Green et al., 2004). The availability of molecular equations for mixed-volatile solvents makes the prediction of phase separation possible; however, in practice, extrapolation of the HKF/DEW formulation to treat non-aqueous solvents is largely untested.

4.4 Open- vs Closed-System Devolatilization

The open-system model corresponds to Rayleigh fractionation of the fluid phase. This simulates a scenario in which fluid generated by sediment devolatilization is lost immediately to the mantle wedge and that the sediments are isolated from any fluids produced at greater depth by channelized flow. The mass-loss for this model (Fig 6c) is roughly an order of magnitude below the solute mass present in the fluid for the closed-system model (Fig 6a), yet the fluid speciation of both models is nearly identical (Fig 5c). Thus the difference between the models is that the open-system mass-loss reflects solubilities at the time of fluid generation. That mica is refractory in the open-system model demonstrates that its dehydration in the closed-system model is due entirely to dissolution. As most fluid generation occurs at low pressure, the open-system mass-loss is dominated by Na and, to a lesser extent, Si and carbonate species.

The lagged fluid speciation in the closed- and open-system models is virtually identical (Fig 5c) at pressures below the rock-dominated limit for the closed-system model (~6.7 GPa). The open-system model does not reach this limit because the removal of sulfur from the system stabilizes

the calculation. Comparison of the open-system fluid speciation with that obtained by back-calculation (Fig 5a) illustrates that use of back-calculated results beyond the rock-dominated limit leads to substantial errors.

By excluding the possibility of fluid infiltration, the open-system model represents the most conservative model for subduction zone mass transfer. Based on the assumptions discussed previously in reference to the closed-system model, Equation 13 yields global carbon losses by fluid fractionation (n_C = 0.05 mol/kg, Fig 6c) of 5.5 Mt/y, of which 1.1 Mt/y is lost at fore-arc depths at the onset of fluid generation. While the uncertainties are formidable, this result suggests that indeed a simple devolatilization-dissolution process cannot explain island-arc carbon emissions in the range 18-55 Mt/y (Kerrick and Connolly, 2001a; Dasgupta and Hirschmann, 2010; Kelemen and Manning, 2015) and that a fluid-mediated explanation for these emissions requires that the crust be infiltrated by fluids derived by mantle dehydration.

4.5 Infiltration-Driven Devolatilization

For the subduction zone thermal model adopted here (Rupke et al., 2004), serpentine dehydration occurs when the slab surface is at pressures between 3.9 and 4.6 GPa (Connolly, 2005). Taking 4.3 GPa as a representative pressure and the metasediment composition obtained from the open-system model at that condition (Table 2), infiltration-driven mass transport is assessed under the assumption that fluid released by serpentine dehydration is, and remains, pure water until it reaches the sediments. This assumption is unlikely to be true for elements such as Na and Si (Galvez et al., 2016), which are abundant in the igneous crust, but it is a reasonable first approximation for K and C which are concentrated in the thin (~1300 m) package of altered basalt and sediment atop the subducted slab (Staudigel et al, 1989; Alt & Teagle 1999). The thinness of this package is taken as justification for reducing the problem to a zero-dimensional model. Models in which the fluid is generated within, and infiltrates through, a

subducted metamorphic column are tractable (Connolly, 2005; Gorman et al., 2006), but too complex for presentation here.

The initial fluid speciation in the zero-dimensional infiltration model (Fig 7b) is slightly different from the speciation for the open-system model (Fig 5c) at the same pressure because the addition of pure water eliminates the small amount of diamond that is ubiquitous in the previous models and stabilizes oxidized sulfur species ($CaSO_4$, HSO_4^-, HSO_3^-). The infiltration model indicates that ~23 mol of water is required to completely decarbonate a kilogram of GLOSS metasediment (Fig 7c). As serpentinized mantle contains ~13 wt % H_2O or 7.2 mol H_2O/kg mantle, this implies a mass of serpentinite ~3.2 times that of the carbon-bearing oceanic crust is adequate to completely decarbonate the crust. This mass is well within estimates for upper limit on the extent of mantle serpentinization (Connolly, 2005).

The elimination of mica and alkali earth elements by the addition of slightly more water than required for decarbonation leaves lawsonite as the only carrier of water at depths beyond the conditions of serpentine dehydration. With continued subduction lawsonite would dehydrate (Fig 4), leaving the metasediment completely depleted in alkali earth elements, and hydrogen and, thereby, refractory to melting. By neglecting the effect of the igneous crust on the chemistry of mantle derived fluid, the present model likely exaggerates Na-depletion. This model defect is less likely to be important for potassium, which correlates strongly with hydrogen, because of its greater solubility and lower absolute abundance in the igneous crust. Thus, the result suggests an anti-correlation between the efficacy of infiltration-driven decarbonation and slab melting. Unfortunately, there are many reasons why slab melting (Behn et al., 2011) is sporadic, and therefore its absence is not an argument for the importance of infiltration-driven decarbonation.

The complete depletion of C, K, and Na in the infiltration-driven model may seem to contradict the lagged speciation rock-dominated limit. This is not the case, as in the simple open-system model, because the elements depleted from the condensed phases are removed from the system by the fluid.

5. Discussion

The lagged-speciation algorithm derives extraordinary efficiency by using back-calculated fluid speciation (Galvez et al., 2015) to predict the stable composition of electrolytic fluids during Gibbs energy minimization. The cost of this efficiency is that the algorithm fails if the predicted fluid composition is inconsistent with mass balance constraints. While there is no remedy for this condition, the conditions can be recognized, making it apparent when reformulation of the solvent model or a more rigorous algorithm (e.g.: Harvie et al., 1987; Karpov et al., 2001) is required. A limitation of the algorithm related to this failing is that it cannot treat situations in which an element is present only in the form of a solute species. In the case C, O, H, and S, which appear both as molecular fluid species and common mineral constituents, this limitation can be circumvented by reformulating the solvent model to include these elements. Halogens are more problematic. There are equations of state that describe brines in terms of a solvent standard state for NaCl (Driesner and Heinrich, 2007; Aranovich et al., 2010; Dubacq et al., 2013), the complication in integrating such equations of state with solute speciation models such as the HKF is to define a relation between the macroscopic and microscopic NaCl content and to account for the resulting non-linearity in activity-composition relations. This complication has not been addressed in the computer implementation of the lagged speciation algorithm. An alternative strategy for treating undersaturated solute components is to introduce an auxiliary condition for the solute component mass (Galvez et al., 2016); however, such a strategy presumes stability of the fluid phase.

In geochemical implementations of the HKF/DEW formulation, water is the sole solvent and molecular volatiles and organic species are described by a solute standard state. In contrast, Galvez et al. (2015) adopted a solvent standard state for the dominant carbonic volatile species. Both solvent formulations offer advantages in specific situations, in the case of a miscible low temperature water-rich solvent phase both formulations produce comparable results (Fig 5b). This agreement deteriorates at higher temperature and, due to the implicit assumption of Henryian behavior in the solute reference state, leads to underestimation of molecular volatile solubilities (Galvez et al., 2016).

Because the primary concern of this paper is methodological, no attempt has been made to assess the accuracy of the thermodynamic data used for the calculations presented here. This data is subject to significant random sources of error, but a bias toward under-prediction of mineral solubility is inherent in microscopic speciation models due to the existence of unanticipated species (Manning, 2007; Pokrovski and Dubrovinsky, 2011; Manning et al., 2010; Tumiati et al., 2017). Sverjensky et al. (2014) demonstrated that the current data is capable of reproducing experimental solubility data in two-component systems at subduction zone pressure conditions; however, in systems with chemistry approaching that of natural rocks, thermodynamic models underestimate the concentrations of Ca, Al, Fe, and Mg by orders of magnitude (Galvez et al., 2015). Although this error is significant, the absolute concentrations of these elements, with the probable exception of Al, is small compared to those of the alkali elements at subduction zone conditions (Tsay et al., 2017).

6. Conclusion

With the aforementioned caveats, accounting for electrolytic fluids does not profoundly change the efficacy of fluid-mediated carbon-loss during subduction based on classical molecular fluid models because carbonic molecular species remain prominent, if not dominant, in electrolytic

fluids. The behavior of sulfur is more surprising. At fore-arc conditions S is nearly insoluble and accommodated primarily as H_2S. The present modeling (Fig 5) suggests that sulfur solubility rises at sub-arc conditions due to the stability of oxidized sulfur species that form by the reduction of carbonate to diamond (Frezzotti et al., 2011). This rise in solubility is intriguing as a mechanism for transferring an oxygen excess to the mantle wedge.

Subduction zone carbon input and output are of the same order of magnitude, but are uncertain by at least a factor of two (Kerrick and Connolly, 2001a; Dasgupta and Hirschmann, 2010; Kelemen and Manning, 2015). Thus, there is no compelling argument that slabs must be completely decarbonated at sub-arc depths. A more important issue is whether it is possible to reject the null hypothesis that sub-solidus decarbonation is adequate to explain island-arc carbon emissions. Earlier studies based on a closed-system devolatilization model (Kerrick and Connolly, 2001ab), which exaggerates the extent of decarbonation, rejected the null hypothesis. Since that time, sub-arc temperature estimates have increased significantly (Syracuse et al., 2010; Penniston-Dorland et al., 2015) with the result the physically unrealistic closed-system model can explain island-arc carbon emissions (Section 4.1). Open-system devolatilization (Section 4.4), the simplest possible physically realistic model, reduces the extent of decarbonation by an order of magnitude, so that it remains plausible to reject the null hypothesis. The intent here has not been to deny or advocate any particular alternative hypothesis, but solely to reexamine the efficacy of infiltration-driven devolatilization.

Gorman et al. (2006) is often cited to support the contention that infiltration-driven devolatilization is incapable of explaining island-arc carbon emissions. However, the behavior in the Gorman et al. (2006) models was influenced by the choice of an anomalously young slab age. Because the top of subducted slabs is heated rapidly after the slab mantle becomes detached from the lithosphere (Rupke et al., 2004), carbon solubility rises to a maximum at

sub-arc depth for typical subduction zone conditions (Connolly, 2005; Galvez et al., 2016; Fig 6 here). Slab age is important in this context because it controls when serpentine dehydration, the putative source of infiltrating fluid, is released. For subduction models based on a slab age close to the global average, there is no difficulty in explaining island-arc carbon emissions in terms of an infiltration-driven scenario for decarbonation (Connolly, 2005). The concern over whether such models are capable of quantitatively explaining decarbonation is misplaced. Rather, the weakness of the infiltration-driven scenario is the assumption that large volumes of mantle-derived fluid equilibrates pervasively with the subducted crust. The value of incorporating electrolytic fluid chemistry in models of infiltration-driven devolatilization is that it offers a complete geochemical picture of the infiltration process and, thereby, may provide arguments for the rejection or acceptance of the mechanism. In particular, the present modeling (Section 4.5) suggests that any sub-solidus infiltration event capable of depleting carbon from the subducted crust would effectively desiccate the crust by potassium depletion and render it refractory with respect to melting. A critical assumption in this argument is that lawsonite is not stable on the fluid-absent solidus (cf., Poli, 2015).

Acknowledgements

Craig Manning inspired and reviewed this paper, which also benefited from the perceptive comments of an anonymous reviewer, the editorial direction of Mike Bickle, and discussions with Terry Plank, Raj Dasgupta, and Peter Kelemen. This work was supported by Swiss National Science Foundation grant 200021_162450.

References

Ague, J.J., Nicolescu, S., 2014. Carbon dioxide released from subduction zones by fluid-mediated reactions. Nat. Geosci. 7, 355-360. https://doi.org/10.1038/ngeo2143.

Aranovich, L.Y., Zakirov, I.V., Sretenskaya, N.G., Gerya, T.V., 2010. Ternary system H2O-CO2-NaCl at high T-P parameters: An empirical mixing model. Geochemistry International 48, 446-455. https://doi.org/10.1134/s0016702910050022.

Bebout, G.E., 1995. The impact of subduction-zone metamorphism on mantle-ocean chemical cycling. Chemical Geology 126, 191-218.

Behn, M.D., Kelemen, P.B., Hirth, G., Hacker, B.R., Massonne, H.J., 2011. Diapirs as the source of the sediment signature in arc lavas. Nat. Geosci. 4, 641-646. https://doi.org/10.1038/ngeo1214.

Bethke, C.M., 1996. Geochemical Reaction Modeling : Concepts and Applications. Oxford University Press Inc, New York.

Canil, D., Fellows, S.A., 2017. Sulphide-sulphate stability and melting in subducted sediment and its role in arc mantle redox and chalcophile cycling in space and time. Earth and Planetary Science Letters 470, 73-86. https://doi.org/10.1016/j.epsl.2017.04.028.

Chatterjee, N.D., Froese, E., 1975. A thermodynamic study of the pseudo-binary join muscovite-paragonite in the system $KAlSi_3O_8$-$NaAlSi_3O_8$-Al_2O_3-SiO_2-H_2O. American Mineralogist 60, 985-993.

Connolly, J.A.D., 2005. Computation of phase equilibria by linear programming: A tool for geodynamic modeling and its application to subduction zone decarbonation. Earth and Planetary Science Letters 236, 524-541.

Connolly, J.A.D., 2009. The geodynamic equation of state: What and how. Geochemistry Geophysics Geosystems 10. https://doi.org/10.1029/2009gc002540.

Dasgupta, R., Hirschmann, M.M., 2010. The deep carbon cycle and melting in Earth's interior. Earth and Planetary Science Letters 298, 1-13. https://doi.org/10.1016/j.epsl.2010.06.039.

Dasgupta, R., Hirschmann, M.M., Withers, A.C., 2004. Deep global cycling of carbon constrained by the solidus of anhydrous, carbonated eclogite under upper mantle

conditions. Earth and Planetary Science Letters 227, 73-85. https://doi.org/10.1016/j.epsl.2004.08.004.

DeCapitani, C., Brown, T.H., 1987. The computation of chemical equilibria in complex systems containing non-ideal solutions. Geochimica Cosmochimica Acta 51, 2639-2652.

Driesner, T., Heinrich, C.A., 2007. The system H2O-NaCl. Part I: Correlation formulae for phase relations in temperature-pressure-composition space from 0 to 1000 degrees C, 0 to 5000 bar, and 0 to 1 X-NaCl. Geochimica Et Cosmochimica Acta 71, 4880-4901. https://doi.org/10.1016/i.gca.2006.01.033.

Dubacq, B., Bickle, M.J., Evans, K.A., 2013. An activity model for phase equilibria in the H2O-CO2-NaCl system. Geochimica Et Cosmochimica Acta 110, 229-252. https://doi.org/10.1016/j.gca.2013.02.008.

Evans, K.A., Tomkins, A.G., Cliff, J., Fiorentini, M.L., 2014. Insights into subduction zone sulfur recycling from isotopic analysis of eclogite-hosted sulfides. Chemical Geology 365, 1-19. https://doi.org/10.1016/j.chemgeo.2013.11.026.

Facq, S., Daniel, I., Montagnac, G., Cardon, H., Sverjensky, D.A., 2014. In situ Raman study and thermodynamic model of aqueous carbonate speciation in equilibrium with aragonite under subduction zone conditions. Geochimica Et Cosmochimica Acta 132, 375-390. https://doi.org/10.1016/j.gca.2014.01.030.

Frezzotti, M.L., Selverstone, J., Sharp, Z.D., Compagnoni, R., 2011. Carbonate dissolution during subduction revealed by diamond-bearing rocks from the Alps. Nat. Geosci. 4, 703-706. https://doi.org/10.1038/ngeo1246.

Fruh-Green, G.L., Connolly, J.A.D., Plas, A., Kelley, D.S., Grobety, B., 2004. Serpentinization of oceanic peridotites: Implications for geochemical cycles and biological activity, in: Wilcock, W.S.D., DeLong, E.F., Kelley, D.S., Baross, J.A., Cary, S.C. (Eds.), Subseafloor Biosphere at Mid-Ocean Ranges, pp. 119-136. https://doi.org/10.1029/144gm08.

Fuhrman, M.L., Lindsley, D.H., 1988. Ternary-Feldspar Modeling and Thermometry. American Mineralogist 73, 201-215.

Galvez, M.E., Connolly, J.A.D., Manning, C.E., 2016. Implications for metal and volatile cycles from the pH of subduction zone fluids. Nature 539, 420-424. https://doi.org/10.1038/nature20103.

Galvez, M.E., Manning, C.E., Connolly, J.A.D., Rumble, D., 2015. The solubility of rocks in metamorphic fluids: A model for rock-dominated conditions to upper mantle pressure and temperature. Earth and Planetary Science Letters 430, 486-498. https://doi.org/http://dx.doi.org/10.1016/j.epsl.2015.06.019.

Gorman, P.J., Kerrick, D.M., Connolly, J.A.D., 2006. Modeling open system metamorphic decarbonation of subducting slabs. Geochemistry Geophysics Geosystems 7.

Green, E., Holland, T., Powell, R., 2007. An order-disorder model for omphacitic pyroxenes in the system jadeite-diopside-hedenbergite-acmite, with applications to eclogitic rocks. American Mineralogist 92, 1181-1189. https://doi.org/Doi 10.2138/Am.2007.2401.

Green, E.C.R., White, R.W., Diener, J.F.A., Powell, R., Holland, T.J.B., Palin, R.M., 2016. Activity-composition relations for the calculation of partial melting equilibria in metabasic rocks. Journal of Metamorphic Geology 34, 845-869. https://doi.org/10.1111/jmg.12211.

Harvie, C.E., Greenberg, J.P., Weare, J.H., 1987. A chemical-equilibrium algorithm for highly nonideal multiphase systems - free-energy minimization. Geochimica Et Cosmochimica Acta 51, 1045-1057. https://doi.org/10.1016/0016-7037(87)90199-2.

Holland, T.J.B., Powell, R., 1998. An internally consistent thermodynamic data set for phases of petrological interest. Journal of Metamorphic Geology 16, 309-343.

Kagoshima, T., Sano, Y., Takahata, N., Maruoka, T., Fischer, T.P., Hattori, K., 2015. Sulphur geodynamic cycle. Scientific Reports 5. https://doi.org/10.1038/srep08330.

Karpov, I.K., Chudnenko, K.V., Kulik, D.A., Avchenko, O.V., Bychinskii, V.A., 2001. Minimization of gibbs free energy in geochemical systems by convex programming. Geochemistry International 39, 1108-1119.

Kelemen, P.B., Manning, C.E., 2015. Reevaluating carbon fluxes in subduction zones, what goes down, mostly comes up. Proceedings of the National Academy of Sciences of the United States of America 112, E3997-E4006. https://doi.org/10.1073/pnas.1507889112.

Kerrick, D.M., Connolly, J.A.D., 2001a. Metamorphic devolatilization of subducted marine sediments and the transport of volatiles into the Earth's mantle. Nature 411, 293-296.

Kerrick, D.M., Connolly, J.A.D., 2001b. Metamorphic devolatilization of subducted oceanic metabasalts: implications for seismicity, arc magmatism and volatile recycling. Earth and Planetary Science Letters 189, 19-29.

Lang, S.Q., Fruh-Green, G.L., Bernasconi, S.M., Brazelton, W.J., Schrenk, M.O., McGonigle, J.M., 2018. Deeply-sourced formate fuels sulfate reducers but not methanogens at Lost City hydrothermal field. Scientific Reports 8. https://doi.org/10.1038/s41598-017-19002-5.

Leal, A.M.M., Kulik, D.A., Smith, W.R., Saar, M.O., 2017. An overview of computational methods for chemical equilibrium and kinetic calculations for geochemical and reactive transport modeling. Pure and Applied Chemistry 89, 597-643. https://doi.org/10.1515/pac-2016-1107.

Manning, C.E., Antignano, A., Lin, H.A., 2010. Premelting polymerization of crustal and mantle fluids, as indicated by the solubility of albite plus paragonite plus quartz in H2O at 1 GPa and 350-620 degrees C. Earth and Planetary Science Letters 292, 325-336. https://doi.org/10.1016/j.epsl.2010.01.044.

Manning, C.E., Shock, E.L., Sverjensky, D.A., 2013. The Chemistry of Carbon in Aqueous Fluids at Crustal and Upper-Mantle Conditions: Experimental and Theoretical Constraints, in: Hazen, R.M., Jones, A.P., Baross, J.A. (Eds.), Carbon in Earth, pp. 109-148. https://doi.org/10.2138/rmg.2013.75.5.

Mason, E., Edmonds, M., Turchyn, A.V., 2017. Remobilization of crustal carbon may dominate volcanic arc emissions. Science 357. https://doi.org/10.1126/science.aan5049.

Penniston-Dorland, S.C., Kohn, M.J., Manning, C.E., 2015. The global range of subduction zone thermal structures from exhumed blueschists and eclogites: Rocks are hotter than models. Earth and Planetary Science Letters 428, 243-254. https://doi.org/10.1016/j.epsl.2015.07.031.

Plank, T., Langmuir, C.H., 1998. The chemical composition of subducting sediment and its consequences for the crust and mantle. Chemical Geology 145, 325-394.

Pokrovski, G.S., Dubrovinsky, L.S., 2011. The S-3(-) Ion Is Stable in Geological Fluids at Elevated Temperatures and Pressures. Science 331, 1052-1054. https://doi.org/10.1126/science.1199911.

Poli, S., 2015. Carbon mobilized at shallow depths in subduction zones by carbonatitic liquids. Nat. Geosci. 8, 633-+. https://doi.org/10.1038/ngeo2464.

Prausnitz, J.M., 1969. Molecular thermodynamics of fluid-phase equilibria. Prentice-Hall, Englewood Cliffs, NJ.

Rupke, L.H., Morgan, J.P., Hort, M., Connolly, J.A.D., 2004. Serpentine and the subduction zone water cycle. Earth and Planetary Science Letters 223, 17-34.

Shock, E.L., Oelkers, E.H., Johnson, J.W., Sverjensky, D.A., Helgeson, H.C., 1992. Calculation of the thermodynamic properties of aqueous species at high-pressures and temperatures - effective electrostatic radii, dissociation-constants and standard partial molal properties to 1000 C and 5 kbar. Journal of the Chemical Society-Faraday Transactions 88, 803-826. https://doi.org/10.1039/ft9928800803.

Skora, S., Blundy, J.D., Brooker, R.A., Green, E.C.R., de Hoog, J.C.M., Connolly, J.A.D., 2015. Hydrous Phase Relations and Trace Element Partitioning Behaviour in Calcareous Sediments at Subduction-Zone Conditions. Journal of Petrology 56, 953-980. https://doi.org/10.1093/petrology/egv024.

Sverjensky, D.A., Harrison, B., Azzolini, D., 2014. Water in the deep Earth: The dielectric constant and the solubilities of quartz and corundum to 60 kb and 1200 degrees C. Geochimica Et Cosmochimica Acta 129, 125-145. https://doi.org/10.1016/j.gca.2013.12.019.

Sverjensky, D.A., Huang, F., 2015. Diamond formation due to a pH drop during fluid-rock interactions. Nature Communications 6. https://doi.org/10.1038/ncomms9702.

Syracuse, E.M., van Keken, P.E., Abers, G.A., 2010. The global range of subduction zone thermal models. Physics of the Earth and Planetary Interiors 183, 73-90. https://doi.org/10.1016/j.pepi.2010.02.004.

Tsay, A., Zajacz, Z., Ulmer, P., Sanchez-Valle, C., 2017. Mobility of major and trace elements in the eclogite-fluid system and element fluxes upon slab dehydration. Geochimica Et Cosmochimica Acta 198, 70-91. https://doi.org/10.1016/j.gca.2016.10.038.

Tumiati, S., Tiraboschi, C., Sverjensky, D.A., Pettke, T., Recchia, S., Ulmer, P., Miozzi, F., Poli, S., 2017. Silicate dissolution boosts the CO2 concentrations in subduction fluids. Nature Communications 8. https://doi.org/10.1038/s41467-017-00562-z.

Wolery, T.J., 1992. A Software Package for Geochemical Modeling of Aqueous Systems: Package Overview and Installation Guide. Lawrence Livermore National Laboratory, Livermore, California.

Figure Captions

Fig 1. Schematic phase relations for the H_2O-CaO-SiO_2 system at a condition such that fluid and stoichiometric wollastonite, lime, and quartz are the only possible phases (see Table 1 for phase notation; H_2O is taken to be the sole component of the solvent). The fluid saturation (green) surface bounds bulk compositions at which no fluid is stable and is coincident with the CaO-SiO_2 join; the solid saturation surface (magenta) bounds bulk compositions at which no solid is stable. In the solute-free system (a), for any general composition, the stable phase assemblage is either lm + wo + water or wo + q + water. In the solute-bearing system (b), finite fields must exist for F, F + lm, F + q, and F + wo (gray-scale shading indicates phase field variance). Lagged speciation is infeasible for bulk compositions that lie within these high variance phase fields. In (c), the infeasible compositions are indicated in blue if infeasibility can be established from the necessary condition that the solids of the phase field contain all the non-solvent components of the system and in red if infeasibility can only be established by the more general sufficient condition discussed in the text.

Fig 2. Phase relations calculated as a function of pressure and temperature by lagged speciation for systems composed of (a) 1 kg H_2O + 10 mol SiO_2 and (b) 20 mol H_2O + 12 mol SiO_2 + 0.5 mol K_2O + 1 mol Al_2O_3 (see Table 1 for phase notation and the Appendix for thermodynamic details). Heavy solid black lines locate univariant phase fields and thin black solid lines locate the boundaries of high variance phase fields, gray-scale shading indicates high variance phase fields mapped by the lagged speciation. The boundaries of the red (mu + q + F) and blue (F) phase fields are defined by the lagged speciation, but the algorithm is infeasible within these fields. Blue shading indicates that infeasibility can be established, in this case trivially, from the necessary condition that the condensed phases contain all the non-solvent components of the system. The blue/red color coding has the same significance as in Fig 1c.

The condition for infeasibility is sensitive to both the fluid mass and solute concentrations; solute concentration cannot be independently controlled, but a reduction in solvent mass expands the range of feasible calculation. The magenta field denotes vapor or vapor-like fluid densities for which the HKF formalism is not fully parameterized and does not extrapolate plausibly (Shock et al., 1992). Solid red and blue contours indicate, respectively, total Si and K molality in the fluid as computed by lagged speciation. Dashed curves and contours indicate phase boundaries and results obtained by simple back-calculation. Simple back-calculation assumes the solute-free phase relations (e.g., as in Fig 1a) and can be done regardless of feasibility conditions. Thus the back-calculated solubility isopleths in the infeasible lagged speciation phase fields are for phase assemblages (coes/stv + F in (a) and mu + san + q + F) that do not satisfy the mass balance constraints of the system.

Fig 3. Geotherm conditions assumed for the subduction zone models (Ruepke et al., 2004).

Fig 4. Volumetric phase proportions during closed-system devolatilization of the GLOSS sediment composition (Table 2) computed by (a) lagged speciation and (b) without taking into account dissolution. The lagged speciation results compare the COHS-solvent model (solid curves) and the H_2O-solvent model (dashed curves) commonly assumed in applications of the HKF/DEW formalism. The fields for small amounts of graphite, potassium feldspar, clinoamphibole, and pumpellyite, which are stable at low pressure, are not labelled. Mineral proportions (not shown) computed for the open-system devolatilization model are essentially identical to those obtained by neglecting dissolution. Phase notation and solution models are summarized in Table 1.

Fig 5. Fluid speciation in various models for the devolatilization of the GLOSS sediment composition. (a) Closed-system devolatilization with the COHS-solvent model, comparing the

lagged (solid curves) and simple back-calculated (dashed curves) speciation. (b) Closed-system devolatilization using lagged speciation, comparing the COHS- (solid curves) and H_2O-solvent (dashed curves) models. (c) COHS-solvent using lagged speciation, comparing open- (diamond symbols) and closed-system (solid curves) devolatilization. In simple back-calculation, fluid speciation is calculated post-hoc from the solute-free phase equilibrium model (Fig 4b), thus the phase proportions and fluid composition violate mass balance. Nonetheless, the back-calculated speciation is accurate to within a factor of two within the rock-dominated limit (i.e., at pressure < ~6.7 GPa).

Fig 6. Mass present in, or removed by, the fluid generated during devolatilization of 1 kg of GLOSS sediment in various models. (a) Closed-system: COHS-solvent, lagged speciation (solid curves) vs COHS molecular fluid (dashed curve for C). (b) Closed-system, lagged speciation: COHS-solvent (solid curves) vs H_2O-solvent (dashed curves). (c) Open-system: COHS-solvent (diamond symbols) vs COHS molecular fluid (circular symbols for C); symbols indicate the points along the subduction path at which fluid was generated. In closed-system models, the mass of a component present in the fluid may decrease with pressure due to changing solubility; in the open-system model, mass loss is irreversible.

Fig 7. Phase proportions (a), fluid speciation (b), and mass loss (c) for the infiltration-driven devolatilization model. Phase notation and solution models are summarized in Table 1.

Tables

Table 1. Mineral notation, formulae and solution model sources (1 - Green et al., 2016; 2 - Holland and Powell, 1998; 3 - Fuhrman and Lindsley, 1988; 4 - Chatterjee and Froese, 1975; 5 - Green et al., 2007). Abbreviations for non-stoichiometric phases are capitalized. See Appendix for condensed phase and fluid species thermodynamic data sources.

Symbol	Solution	Formula	Source
Amph	clinoamphibole	$Ca_{2(y+u+v)}Na_{u+2(w+z)}[Mg_xFe_{1-x}]_{7-3u-2v-4(w+z)}Fe_{2z}Al_{4y+3v+2w}Si_{8-(y+v)}O_{22}(OH)_2$	1
als	aluminosilicate	Al_2SiO_4	
arag	aragonite	$CaCO_3$	
cc	calcite	$CaCO_3$	
coe	coesite	SiO_2	
Cpx	clinopyroxene	$Na_{y+w}[CaMg_xFe_{1-x}]_{1-y-w}Al_yFe_wSi_2O_6$	5
Dol	dolomite	$CaMg_xFe_{1-x}(CO_3)_2$	2
F	fluid		
Fsp	feldspar	$K_yNa_xCa_{1-x-y}Al_{2-x-y}Si_{2+x+y}O_8$	3
Grt	Garnet	$[Fe_xCa_yMg_{1-x-y}]_3[Fe_{1-v}Al_v]_2Si_3O_{12}$	1
ky	kyanite	Al_2SiO_5	
law	lawsonite	$CaAl_2Si_2O_6(OH)_2$	
Lm	lime	CaO	
M	magnesite	$Mg_xFe_{1-x}CO_3$	2
Mlt	melt		
Ms	mica	$K_xNa_{1-x}[Mg_{1-v}Fe_v]_yAl_{3-y}Si_{3+y}O_{10}(OH)_2$	4
mu	muscovite	$KAl_3Si_3O_{10}(OH)_2$	1
Pu	pumpellyite	$Ca_4Mg_xFe_{1-x}[Fe_yAl_{1-y}]_5Si_6O_{21}(OH)_7$	ideal
q	quartz	SiO_2	
san	sanidine	$KAlSi_3O_8$	
stlb	stilbite	$CaAl_2Si_7O_{11}(OH)_{14}$	
Stlp	stilpnomelane	$K_{0.5}[Mg_{1-x}Fe_x]_5Al_2Si_8O_{18}(OH)_{12.5}$	ideal
stv	stishovite	SiO_2	
wo	wollastonite	$CaSiO_3$	

Table 2. Average subducted sediment composition (GLOSS, Plank and Langmuir, 1989). The GLOSS composition has been modified by the addition of sulfur corresponding to the presence of ~0.1 volume % pyrite, the original O_2-content has been recomputed so that the bulk composition is redox neutral. The metasediment composition is the bulk composition obtained at 4.3 GPa from the GLOSS composition by open-system devolatilization (Fig 6c).

	Initial GLOSS Sediment		Metasediment at 4.3 GPa	
	mass fraction, %	mol/kg	mass fraction, %	mol/kg
H_2	0.823	4.085	0.197	0.978
C	0.824	0.686	0.847	0.706
Si	27.621	9.835	29.317	10.439
Al	6.369	2.360	6.802	2.521
Fe	4.112	0.736	4.392	0.786
Mg	1.520	0.625	1.623	0.668
Ca	4.285	1.069	4.551	1.135
Na	1.809	0.787	1.804	0.785
K	1.735	0.444	1.798	0.460
O_2	50.578	15.806	48.322	15.101
S_2	0.323	0.101	0.345	0.108

Graphical Abstract (for review)

Computed phase changes, fluid speciation, and mass loss as a function of water infiltration through metasediment at sub-arc conditions.

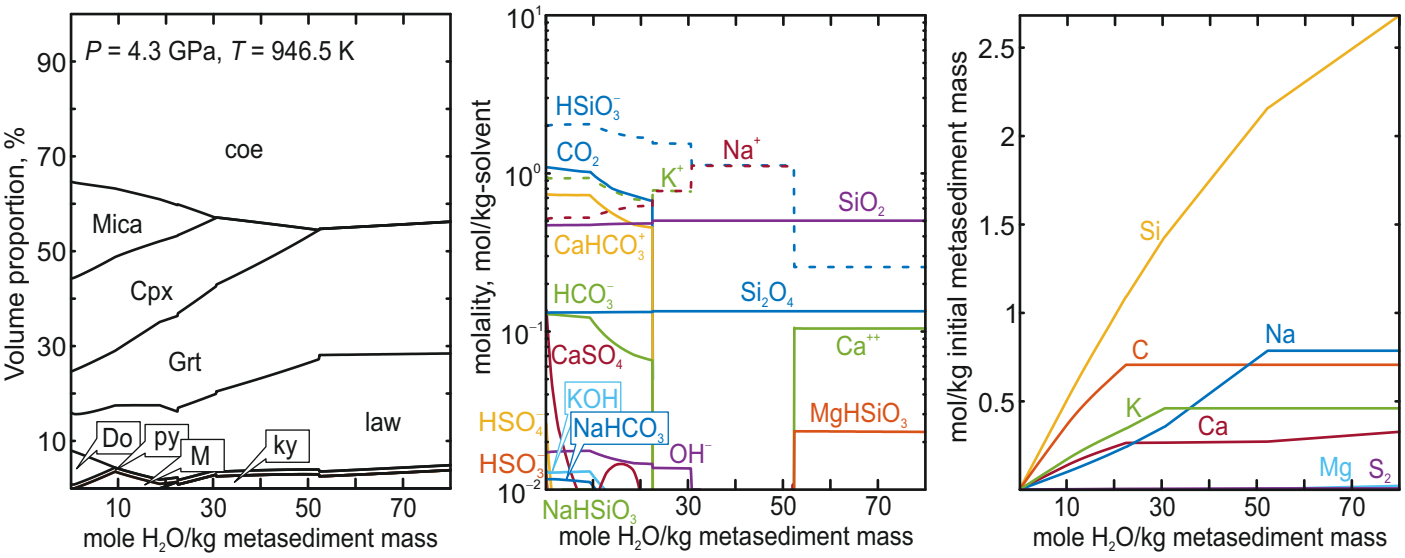

Figure
Click here to download Figure: lagged_figures_revised_I.pdf

Figure 1

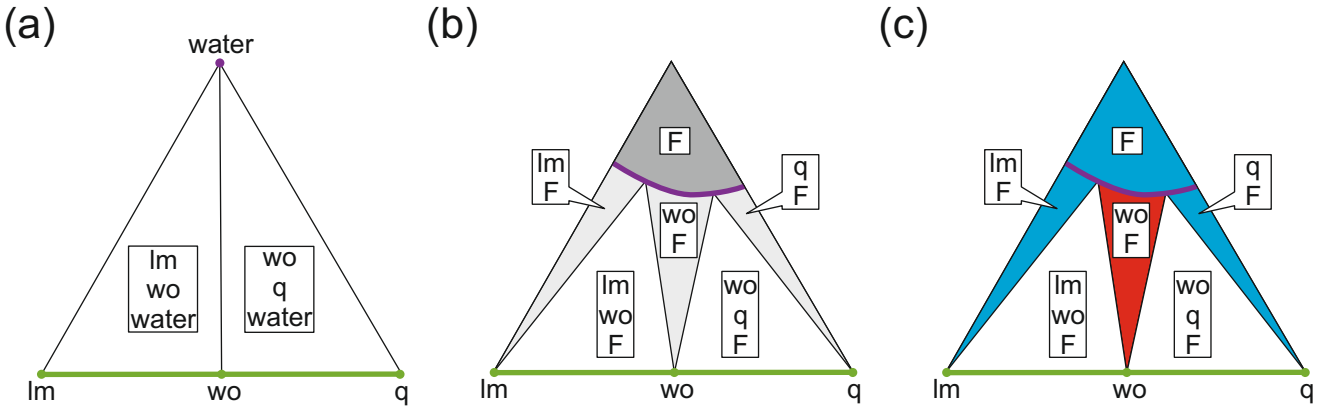

Figure 2

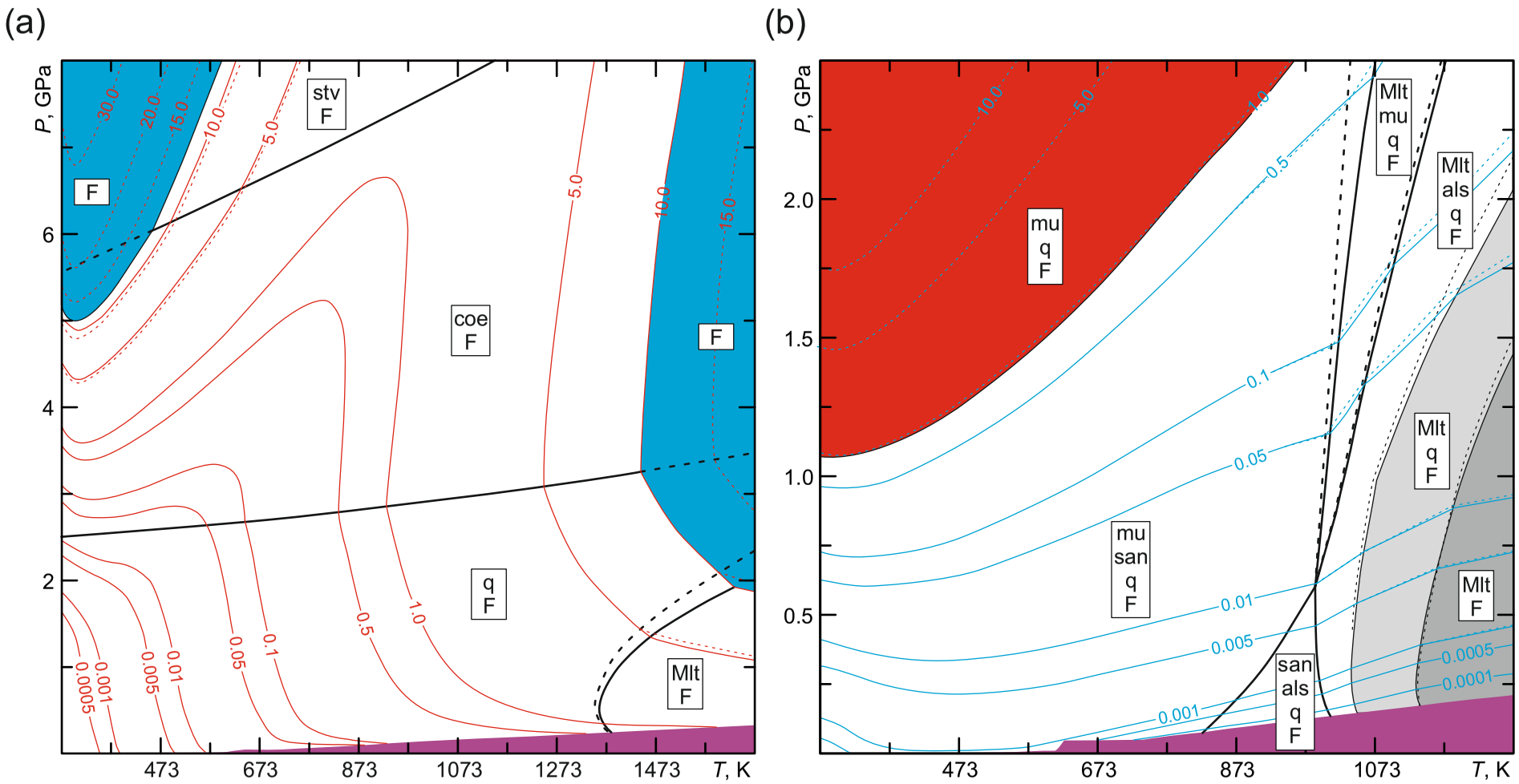
(a)
P, GPa
T, K
F
stv
F
coe
F
q
F
Mlt
F
30.0
20.0
15.0
10.0
5.0
1.0
0.5
0.1
0.05
0.01
0.005
0.001
0.0005
(b)
mu
q
F
mu
san
q
F
Mlt
mu
q
F
Mlt
als
q
F
Mlt
q
F
Mlt
F
san
als
q
F
10.0
5.0
1.0
0.5
0.1
0.05
0.01
0.005
0.001
0.0005
0.0001

Figure 3

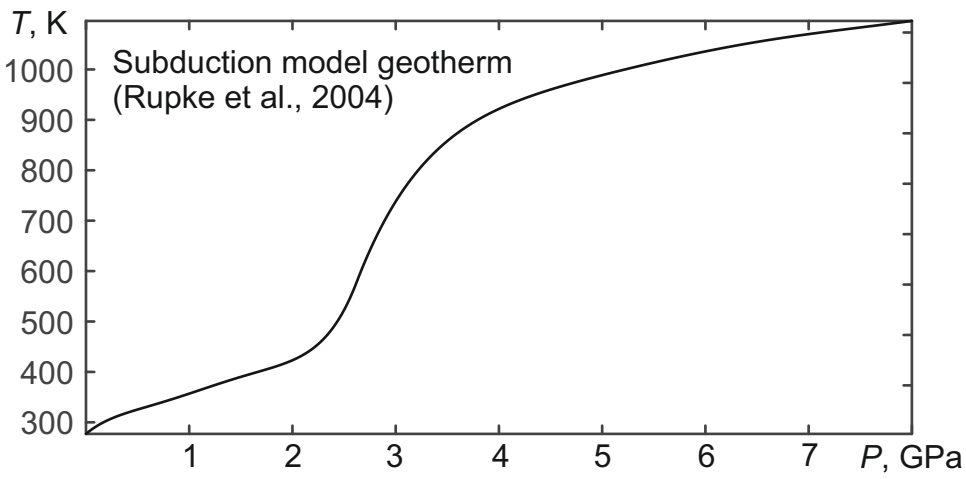
T, K
1000
900
800
700
600
500
400
300
Subduction model geotherm
(Rupke et al., 2004)
1
2
3
4
5
6
7
P, GPa

Figure 4

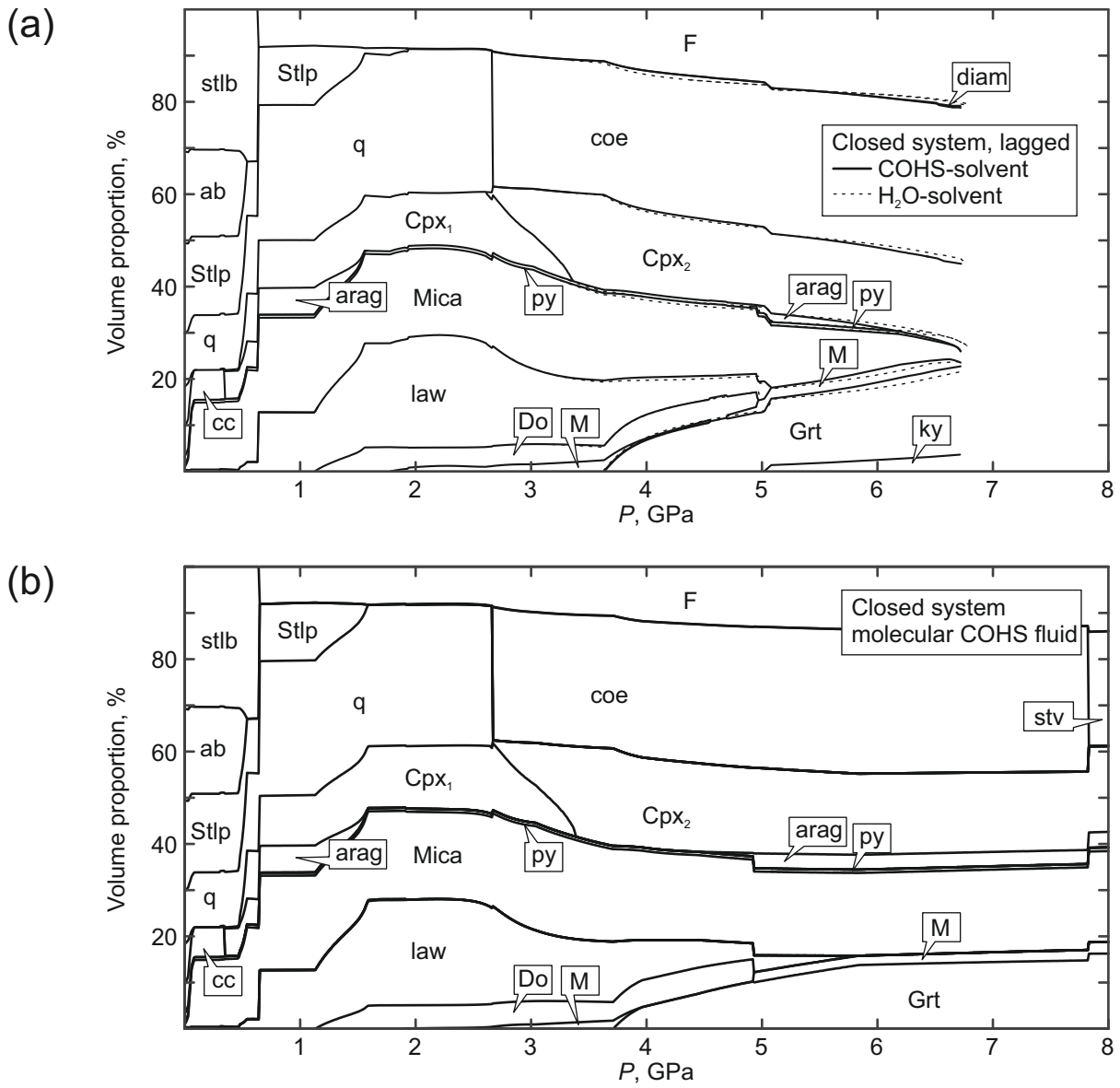
(a)
F
stlb
Stlp
diam
q
coe
Closed system, lagged
COHS-solvent
H2O-solvent
ab
Cpx1
Cpx2
Stlp
arag
Mica
py
arag
py
q
M
law
cc
Do
M
Grt
ky
Volume proportion, %
P, GPa
(b)
F
Closed system
molecular COHS fluid
stlb
Stlp
q
coe
stv
ab
Cpx1
Cpx2
Stlp
arag
Mica
py
arag
py
q
M
law
cc
Do
M
Grt
Volume proportion, %
P, GPa

Figure 5

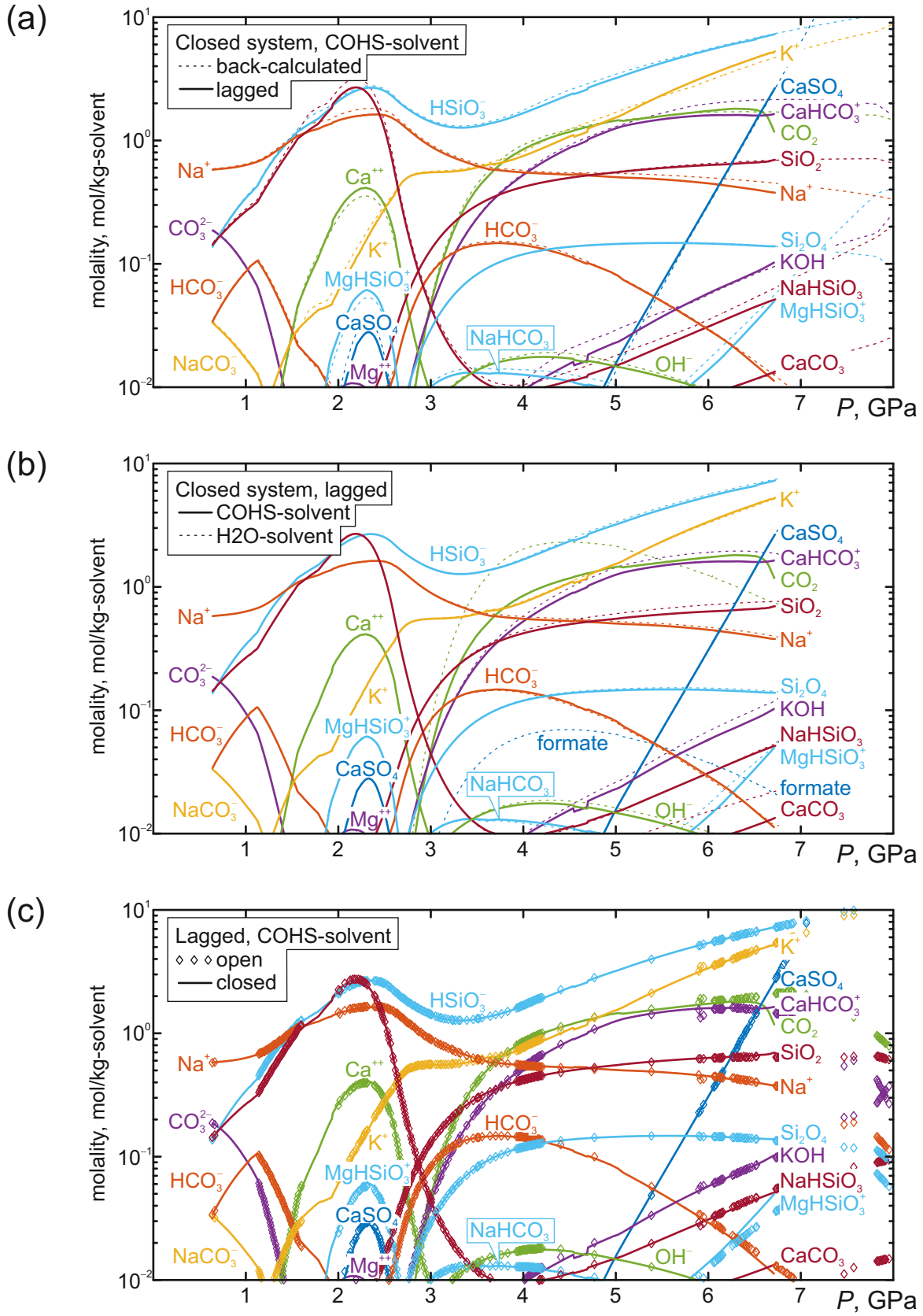
(a)
Closed system, COHS-solvent
back-calculated
lagged
molality, mol/kg-solvent
P, GPa
HSiO3-
Na+
Ca++
CO3 2-
K+
HCO3-
MgHSiO3+
CaSO4
Mg++
NaCO3-
NaHCO3
OH-
CaCO3
KOH
NaHSiO3
MgHSiO3+
Si2O4
SiO2
CO2
CaHCO3+
(b)
Closed system, lagged
COHS-solvent
H2O-solvent
formate
(c)
Lagged, COHS-solvent
open
closed

Figure 6

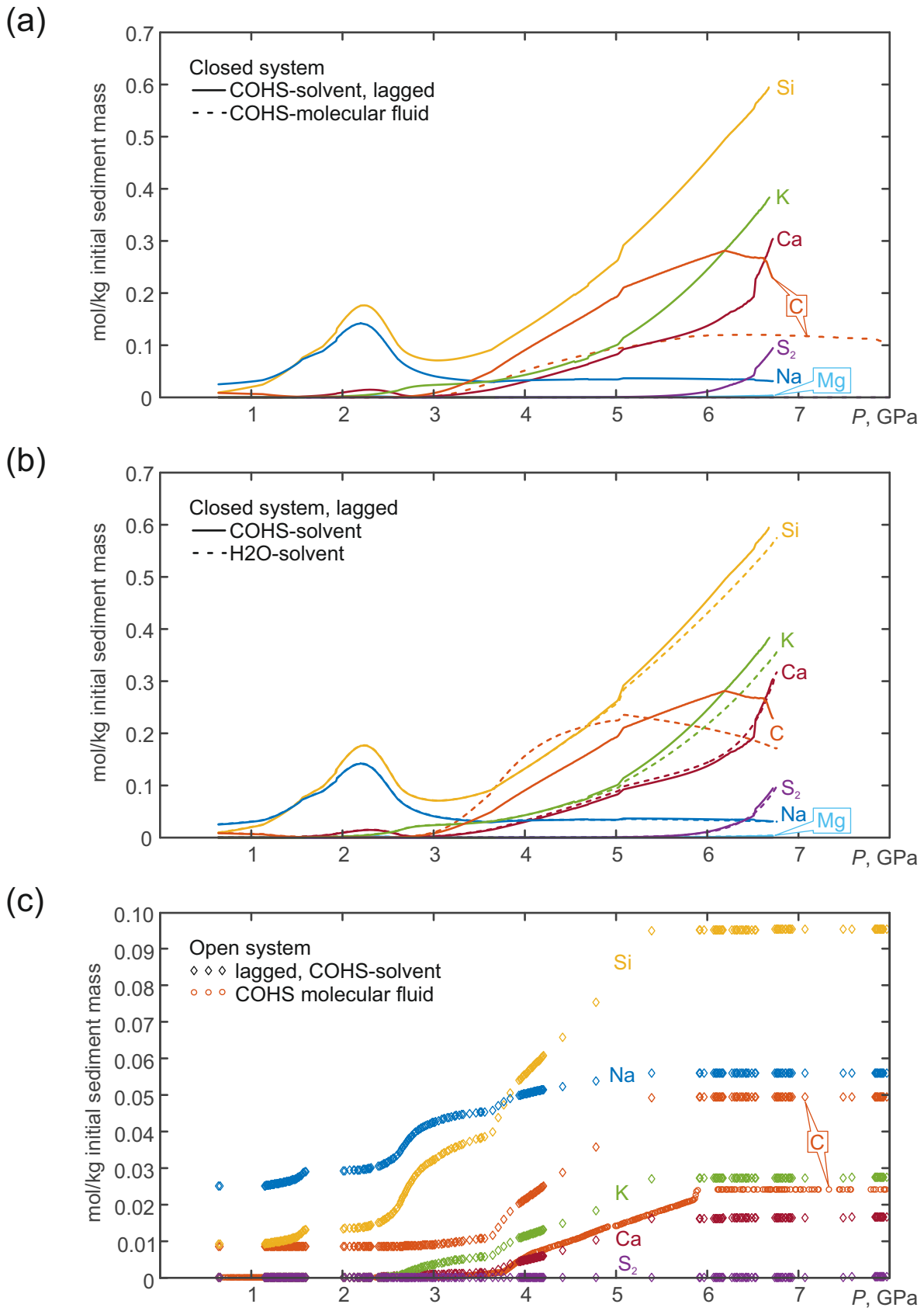
(a)
Closed system
COHS-solvent, lagged
COHS-molecular fluid
mol/kg initial sediment mass
Si
K
Ca
C
S2
Na
Mg
P, GPa
(b)
Closed system, lagged
COHS-solvent
H2O-solvent
mol/kg initial sediment mass
Si
K
Ca
C
S2
Na
Mg
P, GPa
(c)
Open system
lagged, COHS-solvent
COHS molecular fluid
mol/kg initial sediment mass
Si
Na
C
K
Ca
S2
P, GPa

Figure 7

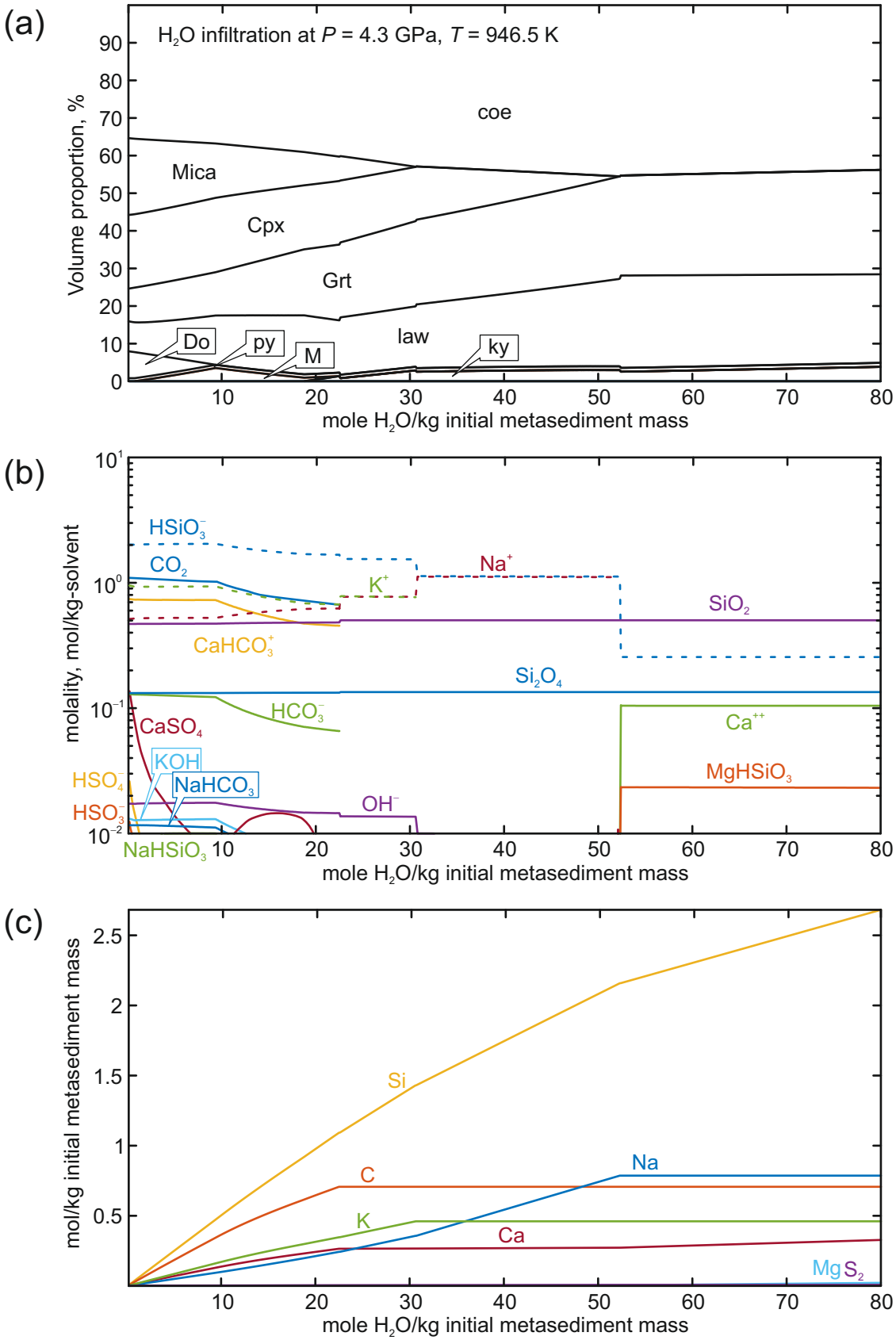
(a)
H2O infiltration at P = 4.3 GPa, T = 946.5 K
Volume proportion, %
coe
Mica
Cpx
Grt
law
Do
py
M
ky
mole H2O/kg initial metasediment mass
(b)
molality, mol/kg-solvent
HSiO3−
CO2
K+
Na+
SiO2
CaHCO3+
Si2O4
HCO3−
CaSO4
Ca++
KOH
MgHSiO3
HSO4−
NaHCO3
HSO3−
OH−
NaHSiO3
mole H2O/kg initial metasediment mass
(c)
mol/kg initial metasediment mass
Si
Na
C
K
Ca
MgS2
mole H2O/kg initial metasediment mass